Stockholm University

Bachelor Thesis

Degree Project in Geochemistry 30 hp

An investigation of methane production in oxygenated surface water during an algal bloom in the Askö area, northern Baltic proper

Fanny Axelsson

Stockholm 2018

Department of Geological Sciences
Stockholm University
SE-106 91 Stockholm

Abstract

Methane concentration maxima in surface waters have been observed in several studies, which contradicts the understanding of methane production occurring strictly in anoxic environments. Various hypotheses of production pathways of the gas in that zone have been presented, but with further research needed to be conducted in the subject. In this bachelor thesis, it is investigated if indications are seen of methane production in the oxygenated surface water in the area of Askö, northern Baltic proper, and if the possible production is effected by the summer algal bloom. Contribution to water-air-fluxes from the possible production and indications of production pathway(s) are also examined. Water samples (profiles and surface waters), incubation experiments, water-air-flux measurements and qualitative analyses of phytoplankton genera were conducted before, during and after the algal bloom in the Askö area. Concentrations of methane, carbon dioxide and nitrous oxide were analysed as well as the isotope composition of the methane. The collected data shows of high concentrations of methane in surface waters with respect to the atmosphere and with increasing methane during the algal bloom: range between ~ 20 - 30 nM at deeper areas and ~ 140 - 150 nM at shallower areas. A concentration maxima within the thermocline was found in one of the sites in June, otherwise, increasing concentrations towards the seafloor were seen. The isotope composition in surface waters was ^{13}C-depleted when compared to methane in the atmosphere, with a range between ~ -60‰ to -55‰ throughout the summer. The water profiles also showed of more depleted methane in surface waters than in bottom waters in most of the months. The methane water-air-fluxes were highest in August at the southern part of Askö, with fluxes up to 5.0 ± 0.4 mg m^{-2} day^{-1} in shallow water areas. Dark incubation experiments (5 weeks long) did not provide any signs of methane production. Conclusions from this investigation is that it is believed that a vertical upward transport of diffusing gas from the sediment was not the only source of methane to the surface water. Two other methane sources are suggested, i) ebullition of ^{13}C-depleted methane from the sediment with bubbles reaching up to the mixed layer: *in situ* at the northern side of Askö as well as at shallower areas at the southern side with further lateral transport to open coastal waters, ii) methane production in the photic zone of the surface water at the southern side of Askö. Further research is needed to be conducted in the Askö area to provide more insights of these hypotheses: light incubation experiments of surface water, data of water currents in the area, isotope composition of methane from diffusion and ebullition from the sediments as well as geophysical acoustic data from ebullition sites.

Bachelor thesis in geochemistry 30 hp
Fanny Axelsson
Supervisors Volker Brüchert at the Department of Geological Sciences at Stockholm University & Helle Ploug at the Department of Marine Sciences at the University of Gothenburg

Table of content

1. Introduction

Methane (CH_4) as an atmospheric greenhouse gas has a contributing role in the research about climate change. The global annual mean of the atmospheric concentration of CH_4 has increased since the beginning of the pre-industrial time from 0.722 ppm in year 1750 (IPCC, 2013) to 1.89 ppm in 2011 (Dlugokencky, 2017). Sources of CH_4 to the atmosphere are from either anthropogenic sources or natural sources, where natural sources include emissions from wetlands, termites, plants, lakes and oceans (Bousquet et al., 2006). Even though there has been extensive research about methane and its emission sources to the atmosphere, the annual global CH_4 budget with sources and sinks is not complete where observed long-term variations in atmospheric concentration is not yet explained (IPCC, 2013).

An on-going debate that could be of use to create further insights of these observed variations regards CH_4 production in oxygenated surface waters. Dissolved CH_4 in oceans and freshwater lakes is produced through biological activity. The production has long been believed to strictly occur in anoxic environments by methanogenic archaea (methanogens) during anaerobic respiration (Ferry, 1993a). Although, concentrations maxima of CH_4 in oxygenated surface waters has regularly been observed. Production processes for CH_4 in the oxygenated zone is not yet understood. Different theories have been presented, but no agreement has been made. One suggestion is interaction between methanogens with either zooplankton (Angelis and Lee, 1995; Karl and Tilbrook, 1994) or phytoplankton (Grossart et al., 2011; Tang et al., 2014), while other theories regards the role of nutrient limitations in the water (Karl et al., 2008; Damm et al., 2010). Several of the observations of high CH_4 concentration in surface waters have been made in freshwater lakes and in high latitude oceans waters. It is therefore of interest to investigate if similar observations can be made in the brackish water of the Baltic Sea. For this bachelor thesis, further examinations are made concerning the theory of CH_4 production due to interaction between methanogens and phytoplankton.

1.1 Aim & hypothesis

The aim of this bachelor thesis is to investigate if there are indications of methane production in oxygenated surface waters due to methanogens-phytoplankton interaction and to analyse if this production of CH_4 significantly contributes to a water-air-flux. It is also of interest to search for indications of production pathway(s) of CH_4 in the waters of the study area. To meet the aims, concentration and isotope composition of CH_4 in water columns were analysed and amount of water-air-fluxes were measured before, during and after the summer algal bloom in the area of Askö, south of Stockholm. Light and dark incubation experiments were conducted to investigate if the CH_4 concentration and isotope composition changed during incubation. Dominating genera of phytoplankton in the surface waters were also examined.

The working hypothesis is that there exists a CH_4 production in the surface waters in the study area that significantly contributes to a CH_4 water-air-flux. The production pathway is believed to be through hydrogenotrophic methanogenesis, where methanogens uses H_2 produced by cyanobacteria. Therefore, the hypothesis is that the methane concentration should increase during the summer algal blooms.

1.2 Background

1.2.1 Water column profiles

Profiles of CH_4 concentrations throughout a water column usually show lower concentrations in the oxygenated surface waters, with increasing concentrations towards bottom waters (Whiticar, 1999). What governs

the distribution of CH_4 in the water column is the CH_4 production by methanogens in the anoxic sediments, which provides a CH_4 flux from the sediment to the water either by diffusion or by ebullition. When CH_4 enters the water column, a vertical transport of CH_4 diffuses the gas upwards. Although, this transport is limited in highly stratified waters and due to aerobic and anaerobic methane oxidation by organisms in the water, the concentration decreases towards the surface (Reeburgh and Heggie, 1977). Similar water profiles have been observed in the Baltic Sea, with surface concentrations of CH_4 < 8 nM and bottom waters > 80 nM (Gülzow et al., 2013). It has also been observed surface waters supersaturated with CH_4, leading to conclusions that the Baltic Sea is a source of CH_4 to the atmosphere (Bange et al., 1994; Gülzow et al., 2013; Schmale et al., 2010).

Regarding the isotope composition of CH_4 in a water column, usually heavier compositions are found in the surface water compared to in the bottom waters. This is due to that production in the sediment provides ^{13}C-depleted CH_4 and when diffusing into the water, oxidation of the gas enriches the CH_4 with $\delta^{13}C$ (Whiticar, 1999). Dissolved CH_4 in the surface water in equilibrium with the atmosphere provides similar values as CH_4 in the gas phase (Knox et. al., 1992).

1.2.2 Methane production pathways

Methanogenesis is the production of CH_4 by methanogens during oxidation of carbon-containing components. There are different pathways for the CH_4 production, meaning that methanogens use different compounds as source of carbon and source of energy to produce methane. The production pathways are hydrogenotrophic methanogenesis (eq. 1) (Mah et al., 1977), acetoclastic methanogenesis (eq. 2) (Gelwicks et al., 1994) and methylotrophic methanogenesis (eq. 3) (Deppenmeier et al., 1996; Penger et al., 2012):

$$4H_2\,(aq) + CO_2 \rightarrow CH_4\,(aq) + 2H_2O \quad \text{(eq. 1)}$$

$$CH_3COOH \rightarrow CH_4\,(aq) + CO_2\,(aq) \quad \text{(eq. 2)}$$

$$4CH_3OH \rightarrow 3CH_4\,(aq) + CO_2\,(aq) + 2H_2O \quad \text{(eq. 3)}$$

In the hydrogenotrophic methanogenesis, hydrogen (H_2) and carbon dioxide (CO_2) are used in the redox reaction to produce CH_4 and water (H_2O) where H_2 is oxidised and CO_2 reduced. For the case of CH_4 production in the surface waters, H_2 is produced during fixation of nitrogen (N_2) by heterocystous cyanobacteria (Bothe et al., 2010). Incubation experiments conducted by Berg et. al (2014) gives support to the hypothesis that methanogens are able to use the produced H_2 from cyanobacteria to further produce CH_4.

In acetoclastic methanogenesis, methanogens use acetate (CH_3COOH) to produce CH_4 and CO_2, where the acetate is produced by bacteria during fermentation of organic matter. The reaction is a redox reaction where the methyl group (CH_3) is being reduced, while the carbonyl group (COOH) is being oxidised (Ferry, 1993b). In the CH_4 production done through methylotrophic methanogenesis, the methanogens use methyl compounds, as for example methanol (CH_3OH). The carbon in the methyl compound forming CH_4 is being reduced, while the carbon forming CO_2 is being oxidised (Deppenmeier et al., 1996).

The isotopic signature from each pathway is difficult to determine accurately (Conrad, 2005). However, studies have shown that methylotrophic methanogenesis is the pathway that fractionates the most, while the acetoclastic methanogenesis the least (Conrad, 2005; Whiticar et al., 1986).

1.2.3 Methane water-air-fluxes

The oceans contain dissolved gases whose solubility depends on temperature, salinity and pressure (Yamamoto et al., 1976). Therefore, in a specific environmental condition a specific amount of gas can be dissolved. The dissolved gas in the water strives to reach an equilibrium with the gas in the atmosphere. This creates a

water-air-flux, where gas is either emitted from the water into the air, and vice versa. With a positive water-air-flux, gas is emitted into the air while with a negative flux, the opposite is happening. Other factors that affects the flux are wind speed, wind direction, surfactants in the water surface, amount of rain and the drop size of the rain, breaking waves and bubbles. What is in common for these factors is that it provides kinetic energy to the water surface and with higher kinetic energy, the flux increases (Ho et al., 1997; Wanninkhof et al., 2009).

1.2.4 Algal bloom in the Baltic Sea: phytoplankton genera

The yearly algal bloom in the Baltic Sea occurs usually in July-August, with warm temperatures and low amount of wind promoting a richer bloom. Therefore, the intensity of the algal bloom varies from year to year with spatial and timely variation (Hansson, 2006). The summer algal bloom consists of phytoplankton cyanobacteria. The capability of the cyanobacteria for nitrogen fixation provides a great advantage when organic nitrogen is depleted during parts of the summer, compared to other phytoplankton that cannot achieve this (Klawonn et al., 2016). The most common cyanobacteria genera during the algal bloom in the area around Askö are *Aphanizomenon spp., Nodularia spp., Dolichospermum spp.* and *Lyngbya spp* (Stal et al., 2003; Wasmund and Uhlig, 2003). As mentioned in section *1.2.3 Methane production pathways*, nitrogen fixation can be coupled with hydrogenotrophic methanogenesis.

1.2.5 Research of methane production in oxygenated surface waters

Several research studies have presented observations of high CH_4 concentration in oxygenated surface waters. The observations have been made in freshwater lakes or in high latitude ocean waters, often in conjunction with the thermocline or with an oxygen concentration maxima. High methane water-air-fluxes have in also been observed in the same studies. Different theories of the production processes of CH_4 have been presented. Already in 1977, Scranton et. al. presented observations of this phenomena and suggested an *in situ* biological pathway for the methane production. Later on, in 1994 Karl & Tillbrook observed methane supersaturation in the surface waters with respect to the atmosphere in the North Pacific Ocean. The study presented a hypothesis that the methane production occurred in the guts of zooplankton, which later was released out to the surface waters by the faecal pellets of the zooplankton. The zone of where the CH_4 concentration maxima was found in that study was in the zooplankton down- and upward migration zone. Another hypothesis that has been suggested is methylotrophic methanogenesis with methylated compounds from degradation of MPn (methylphosphonate) in phosphorous-limited waters (Karl et al., 2008) or from degradation of DMSP (dimethylsulfonio-propionate) in nitrogen-limited waters (Damm et. al., 2010). Although, Grossart et al. (2011) and Tang et. al. (2014) argued against this and suggested that the methane production is performed by oxygen tolerant methanogens through either hydrogenotrophic or aceto-clastic methanogenesis.

Besides CH_4 production, another source of methane into the upper water column is from ebullition from the sediment. The gas bubbles either dissolve in the water column during the ascent or reach the water surface without dissolving, leading to direct emissions into the atmosphere (Schmale et. al., 2005: Schneider von Deimling et al., 2011).

2. Method

Measurements and sampling methods conducted in the field at Askö in June, August and September were i) water sampling, ii) water-air-flux measurements with manual chambers and with an infrared spectrometer, iii) CTD measurements and iv) transect measurements of atmospheric concentration of gases. Water sampling were made throughout water profiles and in surface waters, where some samples were used in an incubation experiment. All samples were analysed for concentration of CH_4, CO_2 and N_2O as well as for isotope composition of $\delta^{13}C_{CH4}$. Some water samples were collected with a plankton net to be used in microscope analysis. To provide a schematic overview of the methods, figure 1 demonstrates each method conducted.

2.1 Study site

The study for this thesis has been conducted in the area of the island Askö at Askö Laboratory (later on referred to as the station). Askö is located south of Stockholm in the northern Baltic proper in the Baltic Sea (figure 2). The surface water in the area has a salinity of approximately 6 - 8‰ (Björck, 1995) and is characterised by stratified water columns with distinct boundary layers from the thermocline and the halocline. There are seasonal differences in the stratification, where mixing within the water column is lower during spring and summer than during winter and fall (Axell, 1998). Stratified waters together with a long residence time of the water in the Baltic sea causes seasonally oxygen deficiency in the bottom waters (Carstensen et al., 2014).

For this study, four sites around the area of Askö were chosen for sampling and measurements: B1, Fifångsdjupet, Julaftons Fyr and Askö. The main focus has been on B1 and Fifångsdjupet where water profiles samples were collected and water-air-flux measurements conducted in June, August and September. An extra site for flux measurement with the infrared spectrometer was chosen in June as well: Tallholmen (58°51'09.66"N, 17°39'25.51"E). No further measurements or sampling were made in that site, though. Overview of which methods used in each site are given in table 1.

The sediment at all sites except at chamber 1 consists of postglacial clay, gyttja clay and/or clay gyttja, while the sediment at chamber 1 is

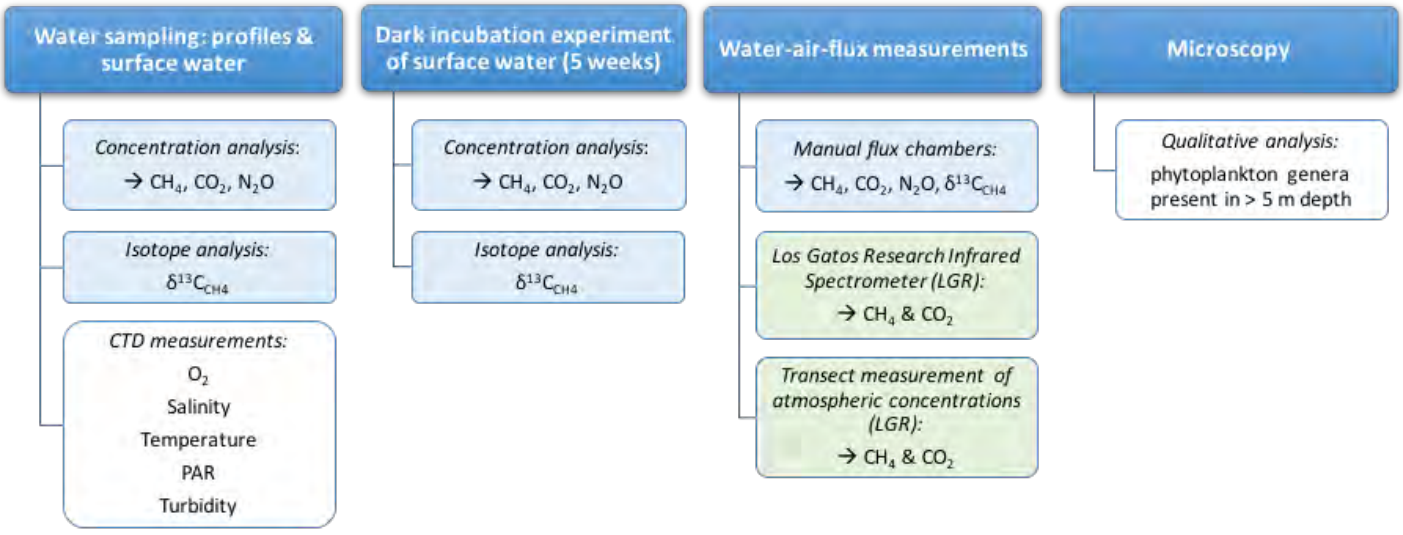

Figure 1. A schematic overview of the methods used to meet the aims of this bachelor thesis.

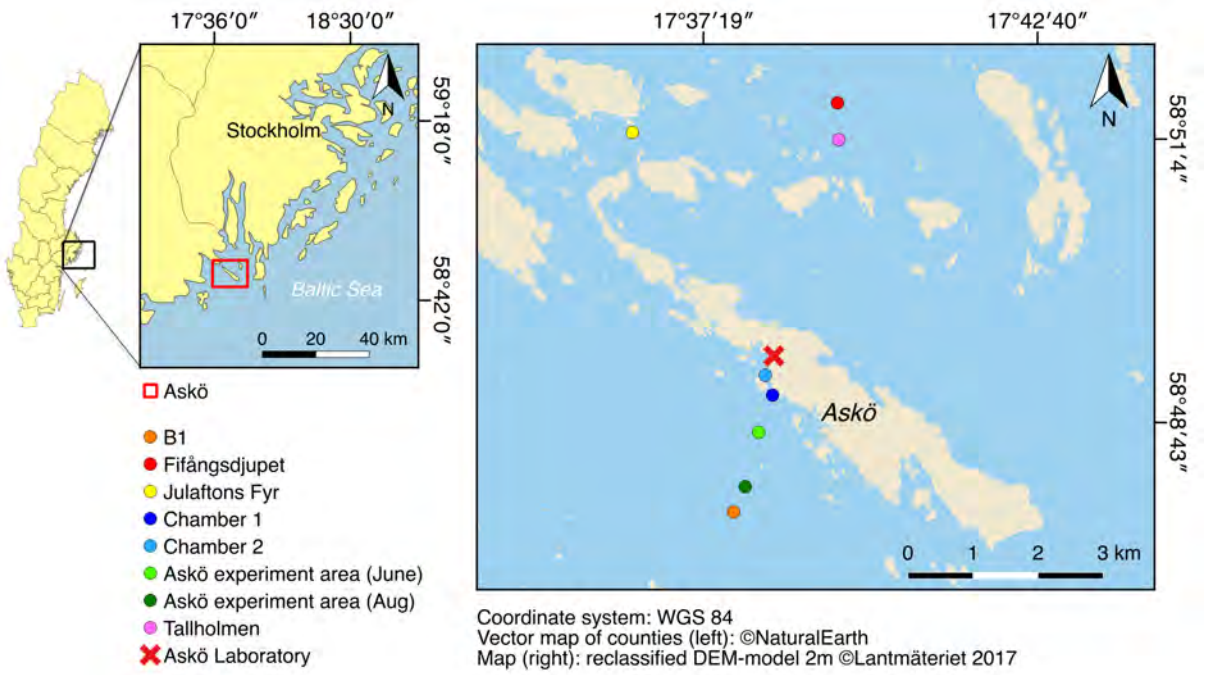

Figure 2. Right: overview map of the location of Askö, south of Stockholm. Left: map of Askö and the sites where sampling and measurements were conducted.

composed of postglacial fine-grained sand (SGU, 2015). In the vicinity of Tallholmen, unpublished data shows that methane ebullition from the sediment occurs, leading to methane release into the water column (E. Weidner, personal communication). It was therefore of interest to choose Fifångsdjupet as a main site, a site with 24 m water depths to the seafloor. The site at B1 (40 m depth to the seafloor) was chosen because it was located in open coastal water of the Baltic Sea, compared to Fifångsdjupet that is located in a more enclosed basin north of the island of Askö (figure 2). It was of interest to see if differences would be seen between the sites due to their locations. Julaftons Fyr (water depth 10 m) was chosen as a sampling site because during field sampling in June anomalously high atmospheric concentration of CH_4 were measured. The site of Askö was chosen for manual flux measurements (depth chamber 1 ~10 m, chamber 2 ~15 m) for examination of fluxes in shallow areas.

2.2 Field methods

2.2.1 Water samples: water profiles, surface water, incubation experiment and microscope samples

Water samples throughout the water column at B1 and Fifångsdjupet and from the water surface at Julaftons Fyr were collected using a 5 L Niskin bottle. The water was poured through a pvc tube into 12 mL exetainers for concentration analysis and into 110 mL glass bottles for isotope analysis. Duplicate or triplicate samples were collected for the concentration analysis and single samples for the isotope analysis. The glass bottles were fitted with a butyl stopper and an aluminium seal. Surface water samples for concentration analysis at the sites of the manual flux chambers were collected with a syringe connected to a PVC tube with the water put into exetainers. Samples for isotope analysis were collected by manually lowering down the sample bottles in the water and filling them avoiding bubble formation. To prevent

Table 1. The table presents the sites and the sampling methods and measurements conducted in each site (conc. = concentrations, iso. = isotope, LGR = Los Gatos Research Infrared Spectrometer, exp. area = experiment area). The red marked depth for B1 for concentration and isotope sampling were the sample depths in June, while in August and September samples were collected from all the depths described in the table.

Site	*Coordinates (WGS 84)*	*Conc. & iso. sample depth (m)*	*Depth plankton net (m)*	*Incubation experiment*	*Air samples*	*LGR*	*CTD*
B1	58°48'18.32"N 17°37'48.32"E	0, 5, 10, 15, 20, 25, 30, 35, 40	5	June, Sep	No	June, Aug, Sep	Yes
Fifångsdjupet	58°51'27.90"N 17°39'25.57"E	0, 9, 18, 22	5	June, Sep	No	June, Aug, Sep	Yes
Julaftons Fyr	58°51′17.35″N 17°36′7.764″E	0	None	No	No	June, Sep	No
Chamber 1	58°49'4.303"N 17°38'12.292"E	0	None	No	Yes	No	No
Chamber 2	58°49'16.032"N 17°38'4.275"E	0	None	No	Yes	June	No
June Askö exp. area	58°48′46.148″N 17°37′57.723″E	None	5	June	No	No	No
Aug. Askö exp. area	58°48'19.519"N 17°37'42.589"E	None	5	Aug	No	No	No

contamination from microbial activity, the concentration samples were poisoned with 100 µL of a zinc chloride solution ($ZnCl_2$, concentration 50%) and isotope samples with 1 mL of 50% $ZnCl_2$.

The samples for the incubation experiment were collected with the Niskin bottle in similar glass bottles as for the isotope analysis and sealed in the same manner. The samples were stored in a cooling room at 15°C for a 5-week-long incubation period. This was made to simulate similar environmental conditions as it was during the sampling. To end the incubation, 1 mL of 50% $ZnCl_2$ was added to the bottles through the stopper with a needle. Further experiments were conducted in June, August and September using a plankton net instead (Appendix 1).

To collect water samples for microscope analysis of phytoplankton genera, a plankton net (4.1 µm) was used. This was lowered down to a depth of 5 m and then poured into a 2 L glass bottle directly on board the research vessel. In the laboratory, the water was poured into glass bottles with 2 mL of lugol (iodine solution) added for separation of the phytoplankton.

2.2.2 CTD: oxygen, salinity, temperature, photosynthetically active radiation and turbidity

The oxygen (O_2) concentration, salinity, temperature, photosynthetically active radiation (PAR = solar radiation between 400-700 nm used in photosynthesis) and turbidity were measured in the water profiles of B1 and Fifångsdjupet with a CTD (Sea & Sun Technology, frequency 4 Hz). Before using the CTD in the field, the O_2 sensor was calibrated by putting the CTD into a bucket of water together with an aquarium pump for > 20 min. The pump caused the dissolved O_2 to equilibrate with the atmosphere. Calibration was made when the O_2 level was stabilised. When using the CTD in the field, the instrument was firstly lowered down ~0.5 m below the water surface for 1 min to adjust. Thereafter, it was sent down with a speed of 25 - 30 cm/sec. The CTD was let to rest

1 min at the bottom before it was pulled back up again. No further analysis was needed for the provided data. However, the results from PAR was used to obtain the euphotic depth, which is the depths of which the PAR value is 1% of the PAR value at the surface (Lee et al., 2007).

2.2.3 Manual flux chambers

Manual flux chambers were placed at two sites, both near the coast of the station (figure 2 and 3: chamber 1 and chamber 2). The same locations were chosen for each occasion in June, August and September. Chamber 1 was placed towards open waters, though still protected from high waves, while chamber 2 was placed in a more enclosed area. 1 - 2 air sample of 50 mL volume were collected each day from the chambers for further analyses of the concentrations of CH_4, CO_2 and N_2O as well as the isotope composition of $\delta^{13}C_{CH4}$. Air samples collected on the first day were taken with a syringe directly from the air to obtain the start values of atmospheric concentration of the gases. The following days, the samples were taken with a syringe connected to a PVC tube. This tube was in return connected via a three-way stopcock to another PVC tube fixed to the chamber. The air samples were injected from the syringe into an upside down-turned 20 mL Wheaton vial (filled with saturated saltwater) through a needle inserted in the lid (butyl stopper with aluminium seal). When doing so, parts of the containing saltwater flowed out through a second needle leaving an overpressure in the vial.

Figure 3. The manual flux chambers floating at the chosen sites: chamber 1 towards open waters and chamber 2 in a more enclosed area.

2.2.4 Los Gatos Research Infrared Spectrometer: flux measurements and atmospheric transects

Measurements of the water-air-fluxes made with an infrared spectrometer (LGR) from Los Gatos Research (model 908-0011-0002, serial 12-0022) were conducted at the sites B1, Fifångsdjupet, Julaftons Fyr and at Askö (in the vicinity of chamber 2). A floating chamber was connected to the instrument via a 26 m long pvc tube (figure 4) (ID 4 mm, OD 7 mm). The research vessel was put at drift and the chamber was placed at the water surface on the side of the boat that allowed the chamber to drift away from the vessel's wind shadow. This was done so that the movement of the boat would not cause any disturbance in the water below the chamber and to minimize the wind field disturbance around the chamber. Concentrations of CH_4, CO_2 and H_2O in the air inside of the chamber were measured with frequencies of either 1 Hz or every 20th second. The time of measurements varied between approximately 5-30 minutes, depending on the rate of the change in concentration inside of the chamber. For faster concentration changes, shorter measurements were done. Some measurements were also aborted after a short period of time due to high input of water vapour into the LGR instrument. During the measurements, information of the air pressure (Pa), the air temperature (K) and wind speed (m/s) were gathered (Appendix 3).

Transects of atmospheric concentration of CH_4 were measured between the sites. The tube was disconnected from the chamber and the end of the tube was placed at the front of the boat to not contaminate the air with exhaust gas from the boat. Coordinates were noted during the transect along with the time and gas concentration. The speed of the boat was 10 knots to make later analyse easier.

Figure 4. Top: The LGR at the boat during a measurement. The graphs display the real-time concentration of the gases. Bottom: The floating chamber connected to the LGR with a 26 m long tube.

2.3 Laboratory & data analysis

2.3.1 Concentration analysis: water samples, incubation experiments & air samples

Analysis were made of the concentrations of CH_4, CO_2 and N_2O in the water samples, incubation experiments and air samples. CO_2 and N_2O were analysed to provide further information regarding biological activity in the water and of greenhouse gas fluxes. The analysis was performed with a gas chromatograph (GC) from SRI 8610C (figure 5: top). The water samples were prepared with a helium headspace > 24 hours before analysis (exetainers = 4 mL, incubation experiment bottles = 16 mL) (figure 5: bottom). The samples were shaken for ~ 22 hours to achieve equilibrium between the gaseous and aqueous phases. 3 mL headspace gas from the exetainers and air samples were extracted for analysis and 2.5 mL from the incubation experiment bottles (the rest left for isotope analysis). When extracting the gas, sea water was simultaneously injected into the exetainers and water saturated with sodium chloride (NaCl) into the incubation experiment bottles. The samples were injected into the GC via two sequential 1 ml loops onto a parallel pair of precolumns (3 feet, Porapak Q) and analytical columns (9 feet, Hayesep D) with carrier gas of nitrogen 5.0 (99.995% purity). A FID (flame ionisation detector) was used to analyse the CH_4, and CO_2, with prior reduction of CO_2 in a

Figure 5. Top: The gas chromatograph (SRI 8610C) used for concentration analysis of CH_4, CO_2 and N_2O. Samples were injected with a syringe. Bottom: Preparation of the helium headspace in an incubation experiment bottle. Water is extracted with a syringe simultaneously as helium is injected.

methaniser. The initial temperature of the FID was 30°C and final temperature of 60°C. An ECD (electron capture detector) determined the N_2O. Calibration curves were made each day by a linear regression from the average peak areas (n = 3 - 10) of a standard with 11.2 ± 0.22 ppm CH_4, 1076 ± 22 ppm CO_2 and 1.07 ± 0.11 ppm N_2O. Air samples obtained from the air outside of the laboratory were used as reference samples to control the quality of the results (concentrations of CH_4 ~ 1,9 ppm, CO_2 ~ 395 ppm and N_2O of ~ 342 ppb previous measured by 2 other instruments). The standard deviation of the total number of measured reference air samples (n = 32) was 7.5%.

The concentration in ppm of the gases were calculated from the calibration curves. To calculate the results into molar concentrations, the following equation was used (Johnson et al., 1990):

$$C_w^\circ = \frac{n_g + n_w}{V_w} \quad \text{(eq. 4)}$$

C_w° = concentration of the dissolved gas in the original sample (moles liter^{-1})
n_g = moles in headspace after equilibration
n_W = moles in aqueous phase after equilibration
V_W = volume of the water sample (liter)

To calculate n_g the ideal gas law was used:

$$n_g = \frac{P * P' * V_g}{RT} \quad \text{(eq. 5)}$$

P = air pressure in the headspace (1 atm)
P' = partial pressure of the gas (ppm value calculated from the peak area multiplied with 10^{-6})
V_g = volume of headspace (liter)
*R = the gas constant (0.08205 atm*L moles*K^{-1})*
T = air temperature during analysis (293 K)

To acquire n_W, firstly the Bunsen solubility coefficient of the dry mole fraction was calculated for each gas (Wiesenburg and Guinasso, 1979):

$$ln\beta = A_1 + A_2\left(\frac{100}{T}\right) + A_3 ln\left(\frac{T}{100}\right) + S\left[B_1 + B_2\left(\frac{T}{100}\right) + B_3\left(\frac{T}{100}\right)^2\right] \quad \text{(eq. 6)}$$

β = Bunsen solubility coefficient (moles liter^{-1} atm^{-1})
S = salinity (set to 6.0‰ for all samples. The difference in the final gas concentration with ±1‰ is negligible)
A and B = coefficients for each gas provided from literature (Appendix 2)

Further on, n_W can be calculated using Henry's Law and the volume of the water (Johnson et al., 1990):

$$n_w = P * P' * K_H * V_w \quad \text{(eq. 7)}$$

K_H = Henry's constant for a specific gas

The relationship between K_H and β is K_H = β/RT (Clark, 2015). Therefore, in the equation used in this thesis the K_H was substituted by β:

$$n_w = \frac{P * P' * \beta * V_w}{RT} \quad \text{(eq. 8)}$$

From the calculated concentrations (C_w°) for each sample, the average concentration and the total standard deviation were calculated from the duplicate and triplicate samples:

$$S_{TOT} = \sqrt{s_s + s_{GC}} \quad \text{(eq. 9)}$$

S_{TOT} = total standard deviation
s_S = standard deviation from the duplicate/triplicate samples
s_{GC} = standard deviation of the GC (7.5%) for the average of the samples (average concentration 0.075)*

Regarding the concentration results of the experiment samples in June obtained from the Niskin bottle at B1 and Fifångsdjupet, these were compared to the results obtained from 0 m depth at the same sites using a two-sided

paired t-test in R Studio calculating a confidence interval (CI) of 95%.

2.3.2 Isotope analysis: water samples, incubation experiments & air samples

The isotope analysis for the water samples in the 110 mL glass bottles, the incubation experiment bottles and for the air samples in the Wheaton vials was made in a gas chromatograph isotope ratio mass spectrometer (GC-IRMS: GC = Trace GC Ultra from Thermo Scientific and IRMS = Delta V Plus from Thermo Electron Corporation). All samples were preconcentrated in a PreCon with loop size of 10 mL for samples with headspace concentration < 25 ppm and a 2 mL loop for samples > 25 ppm (measured previous in the GC described in section *2.3.1 Concentration analysis*). The flow of the carrier gas (helium) in the GC-IRMS was 2.0 mL/min (34 psi), temperature of the combustion oven at 1020°C, GC injector temperature of 150°C and split valve on at 117 mL/min. The reference gas used in the isotope analysis was CO_2 (100%). The average, standard deviation and linearity of the reference gas (n = 8) was measured each day of analysis. Calibration calculations of the $^{13}C/^{12}C$ ratio of the reference gas were made daily from a standard of 100% CH_4. The measurements of the standard were made with direct injections (n = 4) with standard deviation < 0.1 for the calculated $\delta^{13}C_{CH4}$ each day of analysis. In the calibration calculation, the ratio and isotope composition ($\delta^{13}C_{CH4}$) of the reference gas vs. the standard was recalculated into the $\delta^{13}C_{CH4}$ of the reference gas vs. VPDB. Measurement of a standard of 4.96 ± 2.06 ppm (n = 1) in the PreCon was made in the beginning, in the middle and at the end of the day to check the quality of the method. The values were compared with earlier tested values measured by the laboratory staff.

The method for headspace preparation used is described in section *2.3.1 Concentration analysis*. The amount of headspace for water samples analysed with a 10 mL loop was prepared with a 12 mL headspace and samples with a 2 mL loop with 4 mL headspace. Extraction of headspace gas was done with a syringe flushed with argon, where 11 mL gas was used for the 10 mL loop analysis and 3 mL for the 2 mL loop analysis, providing a 1 mL flush of the injection inlet. To obtain the $\delta^{13}C_{CH4}$ vs. VPDB (Vienna Pee Dee Belemnite) of the samples, the following equation was used:

$$\delta^{13}C_{CH4} = \left(\frac{R_S}{R_{VPDB}} - 1\right) * 1000 \quad \text{(eq. 10)}$$

$\delta^{13}C_{CH4}$ = isotope composition of the sample vs. VPDB
R_S = ratio of $^{13}C/^{12}C$ in the sample, calculated from the daily calibrated ratio of the reference gas
R_{VPDB} = given ratio of $^{13}C/^{12}C$ in VPDB

From all of the measurements of the 4.96 ppm standard made in the PreCon during the entire analysis period (n = 20), a standard deviation of the calculated $\delta^{13}C_{CH4}$ from the PreCon was calculated to 0.7%. For single samples, this standard deviation was used to obtain errors of the results. For duplicate and triplicate samples, the total standard deviation was calculated according to equation 9. The results of the experiment samples in June obtained from the Niskin bottle at B1 and Fifångsdjupet were also compared to the results obtained from 0 m depth at the same sites using a two-sided paired t-test.

2.3.3 Data analysis of water-air-fluxes: manual flux chambers & LGR

Manual flux chambers
Water-air-fluxes (mg m^{-2} day^{-1}) of CH_4, CO_2 and N_2O from the manual flux chambers were calculated using the concentrations (ppm) analysed as described in section *2.3.1 Concentration analysis*. Firstly, it was examined how the concentration had changed over time by plotting ppm vs. time. From this, it was shown that equilibrium of the gases was achieved in the chambers after approximately 1 - 2 days after placement of the chambers. Therefore, the air samples collected after the equilibrium was reached were neglected in further description. Firstly, calculation of the

mass of the gases in the chambers for each sample was made:

$$m = \frac{P * P' * V_C * (M * 10^3)}{RT} \quad \text{(eq. 11)}$$

m = mass of the gas (mg)
P = air pressure in the headspace (101 325 Pa)
P' = partial pressure of the gas in the sample (ppm value calculated from the peak area multiplied with 10^{-6})
V_C = volume of the chamber (0.006 m^3)
M = molecular weight of the gas (CH_4 = 16 g $moles^{-1}$, CO_2 = 44 g $moles^{-1}$, N_2O = 44 g $moles^{-1}$) corrected with 10^3 to obtain results in mg
R = the gas constant (8.314 Pam^3 $moles*K^{-1}$)*
T = air temperature during analysis (293 K)

Secondly, to calculate the flux where only 2 samples were collected before reaching equilibrium in the chambers, this equation was used:

$$F = \frac{\frac{m_2 - m_1}{A}}{t_2 - t_1} \quad \text{(eq. 12)}$$

F = water-air-flux (mg m^{-2} day^{-1})
m_2 = mass of the gas from the second air sample (mg)
m_1 = mass of the gas from the first air sample (mg)
A = area of the chamber (0.07069 m^2)
t_2 = day of the second sample
t_1 = 0

To obtain the fluxes where > 2 samples were collected before reaching equilibrium in the chambers, a linear regression analysis was made from the calculated mass of the gas measured from each day (mg day^{-1}). The flux calculation was made by the slope given from the linear regression (*k*):

$$F = \frac{k}{A} \quad \text{(eq. 13)}$$

The standard deviation for the fluxes were calculated from the GC standard deviation of 7.5%.

LGR measurements

The water-air-fluxes of CH_4 and CO_2 from the Los Gatos Research Infrared Spectrometer (LGR) was calculated by firstly converting the measurement time from seconds into days. Secondly, a linear regression analysis was made in R Studio for measurement with normal distributed data to obtain a slope (*k*) of the change in concentration during the measurement from start to end (ppm day^{-1}) and confidence interval (CI) of 95%. For measurements with non-normal distributed data, a bootstrap (resampling) regression analysis were made (replicates = 10 000) to achieve a slope and a basic CI = 95%. This regression has shown to be a valid method to use when having non-normal distributed data (Wang, 2001). Thirdly, the ideal gas law was used to calculate the *k*-value in ppm day^{-1} into moles day^{-1}:

$$k_2 = \frac{P * (k * 10^{-6}) * V}{RT} \quad \text{(eq. 14)}$$

k_2 = slope (moles day^{-1})
P = air pressure during the measurement
k = slope (ppm day^{-1}) corrected with 10^{-6}
V = total volume which includes the chamber volume, the tubes used between the chamber to the LGR and the inside of the LGR (total = 0.006406 m^3)
R = the gas constant (8.314 Pa m^3 $moles*K^{-1}$)*
T = air temperature during the measurement

This equation was also used to calculate the minimum and maximum k_2, where the *k* value was exchanged by the first and third percentile values from the CI. Fourthly, the minimum, average and maximum k_2 values were calculated into water-air-fluxes (mg m^{-2} day^{-1}) with the equation:

$$F = \frac{k_2 * (M * 10^3)}{A} \quad \text{(eq. 15)}$$

The general error of the measurements with the LGR was < 0.01% and therefore disregarded in the calculations of the confidence intervals.

Atmospheric transects

The known coordinates noted during the atmospheric transect measurements together with the CH_4 concentrations at these sites were processed in QGIS. To obtain coordinates for the gas concentration from each specific time measurement, lines were drawn between the known coordinates. The tool "Random points" were used to add the number of measurement points obtained between the known points. The random points were sorted so that each coordinate fitted the right gas concentration at each time measurement.

2.3.4 Qualitative analysis of phytoplankton genera

The water samples for qualitative analysis of phytoplankton genera were examined in an inverted microscope at resolution of 400x. The purpose was to do a qualitative analysis to see which genus dominated in each sample. The number of individuals of the different phytoplankton genera were counted per 1 µL in the microscope. The average and standard deviation of the number of individuals per 1 µL were calculated continuously per sample during the analysis and when the values were stabilised, the analysis was ended.

3. Results

3.1 Water concentrations and isotope composition: water profiles and surface waters

The results are presented in the order of results from the water profile at B1, the water profile at Fifångsdjupet and surface waters at Julaftons Fyr and at the chamber sites. Further details regarding sampling parameters (time, air temperature, weather conditions etc.) during the sampling are presented in Appendix 3.

3.1.1 Water profile: B1

The results from the concentration analysis, isotope analyses and CTD measurements of the water profile at B1 are presented in figure 6 and table 2. The results of the concentration and isotope composition from the depth of 30 m in September is believed to be an analytical anomaly. The suspicion is that water leaked into the Niskin bottle while obtaining the sample. Though, no tests could be executed afterwards to control this suspicion (salinity measurements etc.), so the result is still presented in the graphs.

When observing the results from the various parameters, there are common factors that can be distinguished: i) in August and September, it is seen that changes in O_2 concentration and changes in stable isotope composition ($\delta^{13}C_{CH4}$ vs. VPDB) coincided with the thermocline and the halocline in all three months. The $\delta^{13}C_{CH4}$ changed either above, within or below the thermocline and halocline, with lighter compositions in the surface waters, ii) in September, changes in CH_4 concentration were noted at the same depths as mentioned above, iii) there were seen decreasing values of O_2 concentrations in June and August in the middle of the water column. Changes in O_2 concentration was seen >1 m above the thermoclines in August and September.

June

The thermocline and halocline in June were shown with a temperature drop from 9.8°C to 7.2°C and with a salinity increase from 6.3 PSU to 6.5 PSU between the depths of 9.5 - 10.5 m. Below these depths, the lowest value in O_2 concentration was found at 18 m depth with value of 10.4 mg/L. The $\delta^{13}C_{CH4}$ provided lighter composition above and within the thermocline, compared to below: 10 m = -54.9 ± 0.4‰ versus 20 m = -44.3 ± 0.3‰. The CH_4 concentration showed a significant higher value within the thermocline at 10 m compared to 0 m and 20 m depths: 10 m = 31 ± 3.4 nM versus 0 m = 24 ± 1.9 nM and 20 m = 22 ± 2.4 nM. No significant differences were seen for the concentration of CO_2, though a trend opposite to the CH_4 values are noted. The values were generally higher at 0 m and 20 m and lower at 10 m and 40 m depth. The N_2O concentration was significantly lower at 0 m compared to 20 m and 40 m depth: 0 m = 7.4 ± 0.6 nM versus 20 m = 8.7 ± 0.7 nM and 40 m = 8.9 ± 0.7 nM. The euphotic depth (1% of the surface value of the photosynthetically active radiation (PAR)) was seen at the depth of 28 m. The various times when the CTD measurements were conducted are noted in the PAR-graphs to provide easier interpretation of the PAR-data, with a time for this measurement at 09:00. No distinct differences in turbidity was noted throughout the profile, although, slightly higher values were seen towards the bottom.

August

From the results in August, the thermocline and halocline were found between the depths of 3 - 24 m, with a temperature change from 18.6°C to 6.8°C and salinity from 6.1 PSU to 6.9 PSU. Simultaneously, a decrease in O_2 concentration was found within the thermocline, with lowest concentration at 13 m depth of 7.8 mg/L. A change in the isotope composition was seen within the thermocline. Values at depths ≤ 15 m were more depleted (range between -60.0 ± 0.4‰ to -57.1 ± 0.4‰) than at depth at ≥ 25 m (range between -46.1 ± 0.3‰ to -45.1 ± 0.3‰). The CH_4 concentration showed continuously increasing concentrations towards to seafloor with concentration at 0 m of 32 ± 3.7 nM compared to 40 m of 51 ± 3.8 nM. There were no significant differences within the profile in

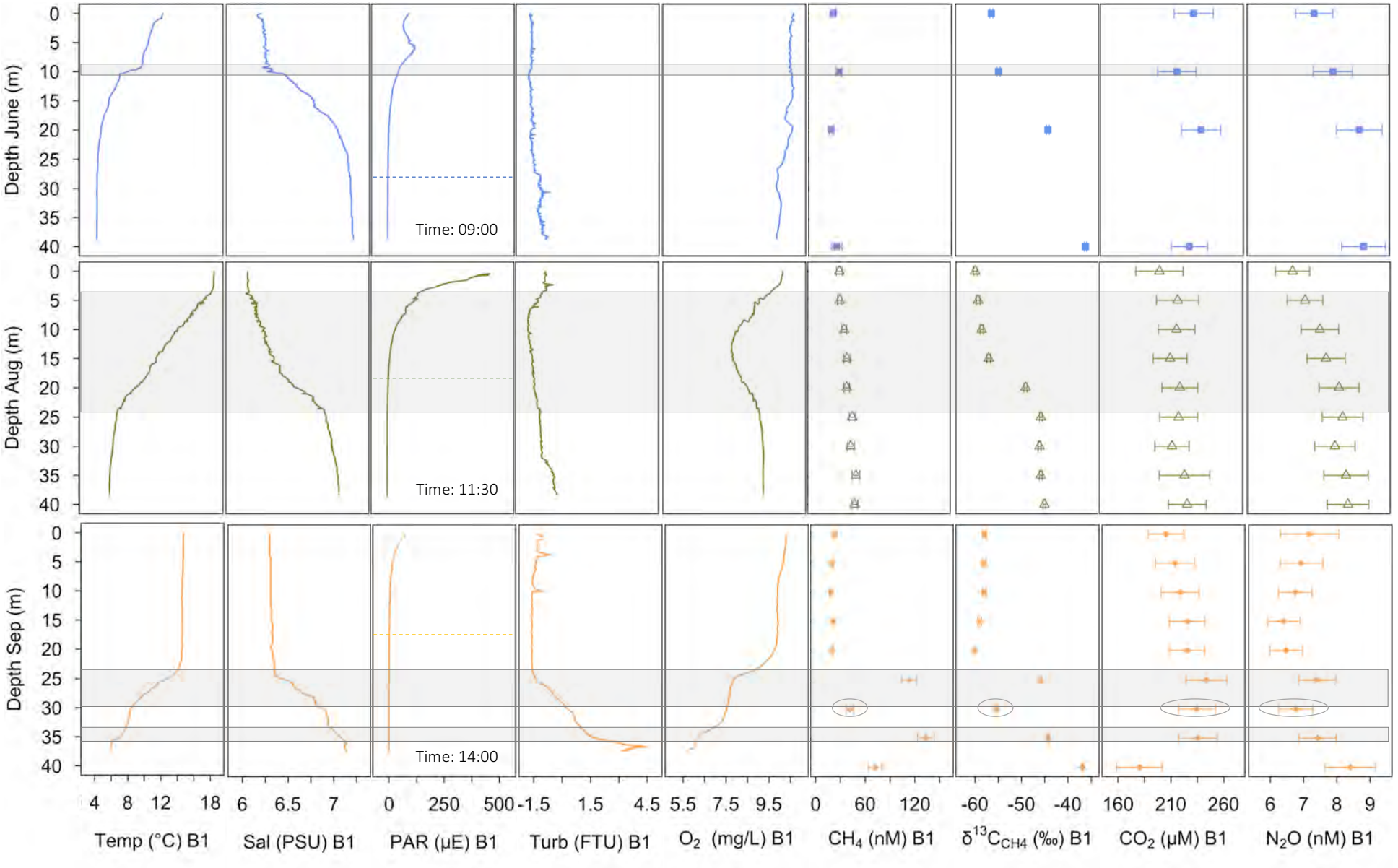

Figure 6. Results of the water profile at B1 from the concentration analysis (CH_4, CO_2, N_2O), isotope analysis ($\delta^{13}C_{CH4}$ vs. VPDB) and CTD measurements (O_2, temperature, salinity, photosynthetically active radiation (PAR), turbidity). Each row shows the three different months, where row 1 = June, row 2 = August and row 3 = September. Each column shares the same x-axis. Error bars represents the standard deviation. The shaded boxes highlight the thermocline in each month and the dashed lines in the PAR-graphs shows the euphotic depths. The time of the CTD measurement is also noted in the PAR-graphs. The circled results at 30 m depth in September are the values suspected to be contaminated.

Table 2. Results from the water profile at B1 in J = June, A = August and S = September for CH_4, $\delta^{13}C_{CH4}$, CO_2 and N_2O (average ± standard deviation). In the comment column: D = duplicate samples, T = triplicate samples, A = analytical anomaly.

Depth B1	*CH_4 (nM) (aver. ± stand. dev.)*	*$\delta^{13}C_{CH4}$ (‰) (aver. ± stand. dev.)*	*CO_2 (µM) (aver. ± stand. dev.)*	*N_2O (nM) (aver. ± stand. dev.)*	*Comments*
0	J: 24 ± 1.9 A: 32 ± 3.7 S: 23 ± 2.3	J: -56.4 ± 0.4 A: -60.0 ± 0.4 S: -58.0 ± 0.4	J: 230 ± 18 A: 200 ± 22 S: 200 ± 17	J: 6.8 ± 0.6 A: 6.7 ± 0.5 S: 7.2 ± 0.9	D T T
5	A: 32 ± 2.5 S: 20 ± 1.6	A: -59.4 ± 0.4 S: -58.1 ± 0.4	A: 220 ± 20 S: 210 ± 18	A: 7.1 ± 0.5 S: 6.9 ± 0.7	T T
10	J: 31 ± 3.4 A: 38 ± 3.2 S: 19 ± 2.1	J: -54.9 ± 0.4 A: -58.6 ± 0.4 S: -58.1 ± 0.4	J: 220 ± 18 A: 220 ± 17 S: 220 ± 18	J: 7.4 ± 0.6 A: 7.5 ± 0.6 S: 6.7 ± 0.5	D T T
15	A: 41 ± 3.5 S: 21 ± 2.9	A: -57.1 ± 0.4 S: -59.0 ± 0.4	A: 210 ± 16 S: 230 ±17	A: 7.7 ± 0.6 S: 6.4 ± 0.5	T T
20	J: 22 ± 2.4 A: 41 ± 3.3 S: 20 ± 1.6	J: -44.3 ± 0.3 A: -49.1 ± 0.3 S: -60.1 ± 0.4	J: 240 ± 19 A: 220 ± 17 S: 230 ± 17	J: 8.1 ± 0.7 A: 8.1 ± 0.6 S: 6.5 ± 0.5	D D D
25	A: 48 ± 3.6 S: 110 ± 9.2	A: -45.9 ± 0.3 S: -46.0 ± 0.3	A: 220 ± 18 S: 240 ±19	A: 8.2 ± 0.6 S: 7.4 ± 0.6	D D
30	A: 46 ± 3.2 (S: 41 ± 4.4)	A: -46.1 ± 0.3 (S: -55.4 ± 0.4)	A: 210 ± 16 (S: 230 ± 18)	A: 8.0 ± 0.6 (S: 6.8 ± 0.5)	D D, A
35	A: 52 ± 4.7 S: 130 ± 10	A: -45.9 ± 0.3 S: -44.3 ± 0.3	A: 230 ± 24 S: 240 ± 18	A: 8.3 ± 0.7 S: 7.4 ± 0.6	D D
40	J: 28 ± 6.1 A: 51 ± 3.8 S: 72 ± 8.3	J: -36.2 ± 0.2 A: -45.1 ± 0.3 S: -37.0 ± 0.3	J: 230 ± 18 A: 230 ± 18 S: 180 ± 22	J: 8.2 ± 0.7 A: 8.4 ± 0.6 S: 8.4 ± 0.8	D D D

the CO_2 concentration. The values ranged from surface concentration of 200 ± 22 µM to bottom concentrations of 230 ± 18 µM. The N_2O concentration was higher in the bottom waters with 6.7 ± 0.5 nM at 0 m depths and 8.3 ± 0.6 nM at 40 m depths. The euphotic depth was also found within the thermocline and halocline at a depth of 19 m (at 11:30) as well as a decline in turbidity at 7.5 m.

September

In September, two boundaries of the thermocline and the halocline were seen that coincided with changes in O_2 concentration, isotope composition and CH_4 concentration. The upper boundaries were found between 22 - 30 m and the lower between 33 - 36 m. Within each part, a decline in O_2 concentration and changes of $\delta^{13}C_{CH4}$ and CH_4 concentration was seen. The total change from the upper part of the first thermocline/halocline to the lower part of the second thermocline/halocline was: temperature = 14.8 - 5.9°C, salinity = 6.3 - 7.1 PSU, O_2 = 10.3 - 5.7 mg/L. The $\delta^{13}C_{CH4}$ became lighter between the depths 0 - 20 m, from -58.0 ± 0.4‰ to -60.1 ± 0.4‰, respectively. Thereafter, it distinctively changed to -46.0 ± 0.3‰ at 25 m depth, while it was even heavier at 40 m depths of -37.0 ± 0.2‰. The CH_4 concentration provided values within the same range between 0 - 20 m: from 23 ± 2.3 nM to 20 ± 1.6 nM. At 25 m depth, it sharply increased to 110 ± 9.2 nM, while it thereafter decreased to 72 ± 8.3 nM at 40 m depths. The concentration of CO_2 showed an increasing trend (with no significant differences) from surface water to 25 m depth: from 200 ± 17 µM to 250 ± 19 µM. This trend ceased at 35 m, while the concentration decreased at 40 m depth to 180 ± 22 µM. A similar, but opposite trend was seen for the N_2O concentration. It decreased from 7.2 ± 0.9 nM at 0 m to 6.5 ± 0.5 nM at 20 m, while higher values were seen at 25 and 35 m depth. Then a second increase was seen at 40 m depth to 8.4 ± 0.8 nM. The euphotic was found at 17 m depth (at 14:00). The turbidity

increased sharply below the thermocline, which indicates of a strong thermocline.

When comparing the three months to each other, it is seen that the thermocline and halocline was weakest in August compared to the other months. The upper mixed layer was 10 m in June, 3 m in August and 22 m in September. Highest vales in the surface waters (≥ 20 m) was found in August and lowest in September. Though, in the bottom waters in September showed highest values and June the lowest. The $\delta^{13}C_{CH4}$ showed similar trends for all three months, where the surface water was lighter than the bottom waters. However, August showed generally lightest values throughout the column and June the heaviest, with a few exceptions. No differences were seen in the CO_2 concentration, except at 40 m depth, where September concentration was lower than the other months. For the N_2O concentration, September provided lower values than June at 10 m depth as well as lower than both June and August at 15 and 20 m.

3.1.2 Water profile: Fifångsdjupet

The results from the concentration analysis, isotope analysis and CTD measurements from the water profile at Fifångsdjupet are presented in figure 7 and table 3. Similar results are shown as presented for B1: i) changes in CH_4 concentration, isotope composition and O_2 concentration coincided with the thermocline and halocline, ii) two boundaries of the thermocline was seen in August, as in September at B1, iii) there was decreasing O_2 concentration in June in the middle of the water column, as seen in June and August at B1, with decreasing concentration >1 m above the thermoclines iv) isotope composition was lighter in surface waters than in bottom waters in June and September. Noteworthy, the ranges of isotope composition throughout the profiles are narrower at Fifångsdjupet than at B1. No pronounced haloclines as normally observed was seen, only slightly increased values in June and August and with a sharp decrease within the thermocline in September.

June

The thermocline in June was found between 7.5 - 10 m depth, with a temperature decrease from 12.5°C to 8.0°C. Within the thermocline at 8 m depth, an increase of the salinity from 6.1 PSU was found as well as decreased O_2 concentration within the thermocline with lowest value of 9.0 mg/L. The CH_4 concentration increased below the thermocline (0 m = 18 ± 1.9 nM vs. 22 m = 35 ± 2.8 nM), while the $\delta^{13}C_{CH4}$ within the thermocline was lighter than the upper and lower samples, with value at 9 m depth of -57.5 ± 0.4‰. The sample at 0 m depth showed similar composition as the bottom samples. The CO_2 concentration did not differ significantly, although, the bottom values showed of generally higher values: 0 m = 220 ± 19 µM vs. 22 m = 230 ± 20 µM. Similar shape of the profile seen in the $\delta^{13}C_{CH4}$ graph is also seen in the N_2O graph, with generally lower concentration at 9 m depth within the thermocline (7.7 ± 0.6 nM) than at the surface and in the bottom. However, no significant differences were seen. The euphotic depth was found at 14 m depth (at 11:00) and with a higher turbidity noted within the thermocline.

August

In August, two distinct thermoclines were seen, the first between 7 - 9 m with a temperature drop from 18.5°C to 17°C. The second were found between 11 - 12.5 m, where the temperature decreased from 16.3°C to 13.5°C. Slightly small changes within these depths was also seen for the salinity: firstly, an increase from 6.1 to 6.2 PSU and thereafter an increase up to 6.3 PSU at 12.5 m depth. The O_2 concentration decreased within both thermoclines, from 9.7 mg/L in the surface water until stabilised at 12.5 m depth at 5.6 mg/L. The CH_4 concentration increased below the thermocline, from 21 ± 1.9 nM at 9 m depth to 57 ± 5.0 nM at 18 m depth, while the $\delta^{13}C_{CH4}$ showed lighter values at 9 m depth of - 57.7 ± 0.4‰ and at 18 m depth -60.1 ± 0.4‰. The CO_2 concentration was similar between 0-18 m depth (~200 ± 15 µM), while a trend of lower concentration was seen at 22 m depth of 190 ± 14 µM. The N_2O concentration was significantly higher at 18 m depth (8.2 ± 0.6 nM) than at 0 m (6.8 ± 0.5 nM) and 9 m depth (6.9 ± 0.5 nM). The euphotic depth was found at 12 m depth (at

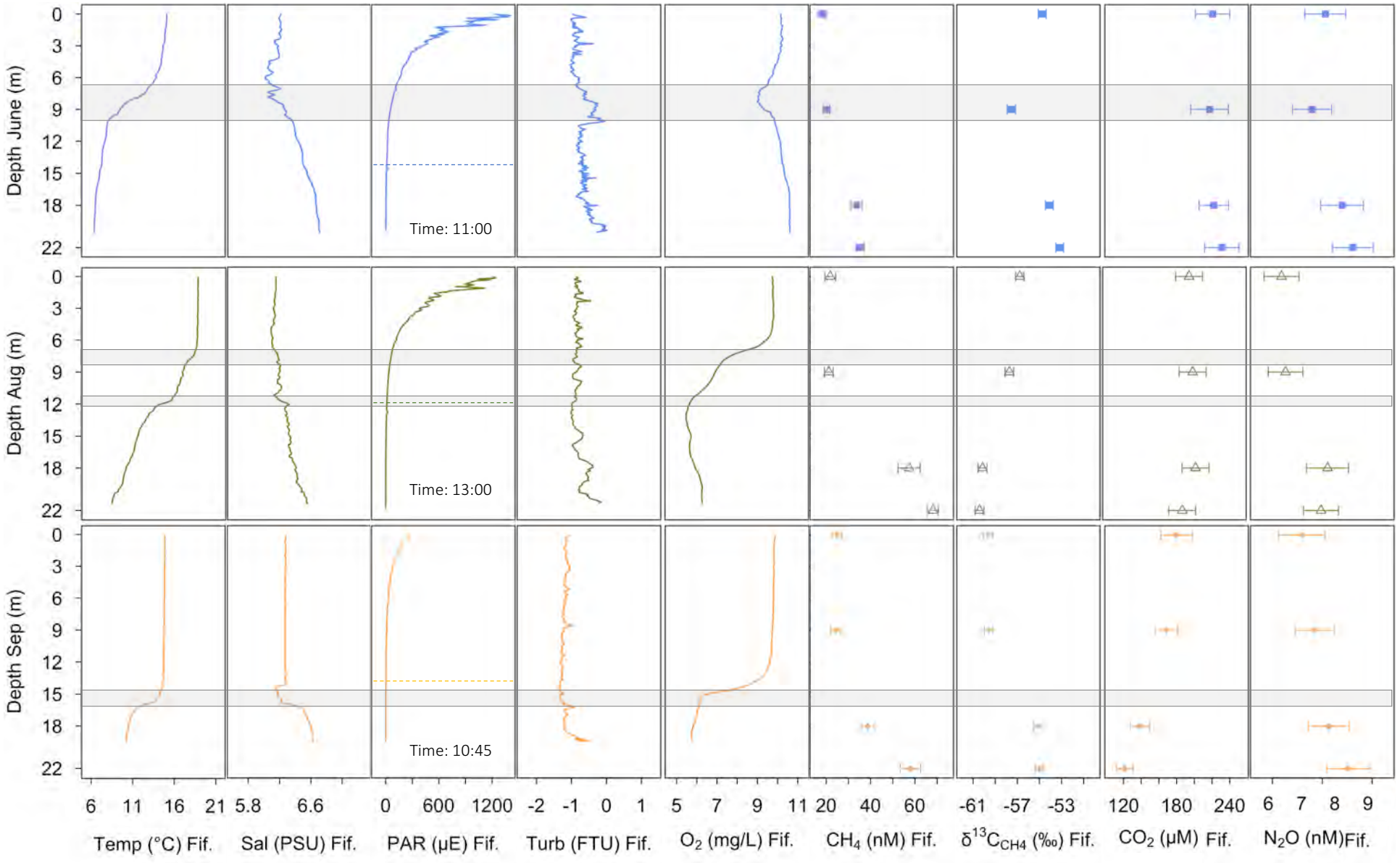

Figure 7. Results of the water profile at Fifångsdjupet from the concentration analysis (CH_4, CO_2, N_2O), isotope analysis ($\delta^{13}C_{CH4}$ vs. VPDB) and CTD measurements (O_2, temperature, salinity, photosynthetically active radiation (PAR), turbidity). Each row shows the three different months, where row 1 = June, row 2 = August and row 3 = September. Each column shares the same x-axis. . Error bars represents the standard deviation. The shaded boxes highlight the thermocline in each month and the dashed lines in the PAR-graphs shows the euphotic depths. The time of the CTD measurement is also noted in the PAR-graphs.

Table 3. Results from the water profile at Fifångsdjupet in J = June, A = August and S = September for CH_4, $\delta^{13}C_{CH4}$, CO_2 and N_2O (average ± standard deviation). In the comment column: D = duplicate samples, T = triplicate samples.

Depth Fif.	*CH_4 (nM) (aver. ± stand. dev.)*	*$\delta^{13}C_{CH4}$ (‰) (aver. ± stand. dev.)*	*CO_2 (µM) (aver. ± stand. dev.)*	*N_2O (nM) (aver. ± stand. dev.)*	*Comments*
0	J: 18 ± 1.9	J: -54.7 ± 0.4	J: 220 ± 19	J: 8.1 ± 0.6	T
	A: 22 ± 2.5	A: -56.8 ± 0.4	A: 200 ± 15	A: 6.8 ± 0.5	T
	S: 25 ± 2.3	S: -59.7 ± 0.4	S: 180 ± 18	S: 7.4 ± 0.7	T
9	J: 20 ± 1.5	J: -57.5 ± 0.4	J: 220 ± 21	J: 7.7 ± 0.6	D
	A: 21 ± 1.9	A: -57.7 ± 0.4	A: 200 ± 15	A: 6.9 ± 0.5	T
	S: 24 ± 2.3	S: -59.6 ± 0.4	S: 170 ± 13	S: 7.8 ± 0.6	T
18	J: 34 ± 2.5	J: -54.1 ± 0.4	J: 220 ± 17	J: 8.6 ± 0.6	D
	A: 57 ± 5.0	A: -60.1 ± 0.4	A: 200 ± 15	A: 8.2 ± 0.6	D
	S: 39 ± 2.9	S: -55.1 ± 0.4	S: 140 ± 11	S: 8.2 ± 0.6	D
22	J: 35 ± 2.8	J: -53.2 ± 0.4	J: 230 ± 20	J: 8.9 ± 0.7	D
	A: 68 ± 5.1	A: -60.4 ± 0.4	A: 190 ± 14	A: 8.0 ± 0.6	D
	S: 58 ± 4.6	S: -55.0 ± 0.4	S: 120 ± 9	S: 8.8 ± 0.7	D

13:00). No distinct changes in turbidity was seen within the profile.

September

The thermocline in September was between 15 - 16.5 m, with temperature decrease from 14.3°C to 11.0 °C. Notably, the salinity showed decreased values within these depth with lowest value of 6.1 PSU and highest of 6.5 PSU. The O_2 concentration was found to be stabilised within these depth at 5.6 mg/L from previous surface values of 9.7 mg/L. The CH_4 concentration and the $\delta^{13}C_{CH4}$ showed higher concentration and heavier composition below the thermocline: 9 m = 24 ± 2.3 nM and -59.6 ± 0.4‰ vs. 18 m = 39 ± 2.9 nM and -55.1 ± 0.4‰. The opposite was seen in the CO_2 concentration compared to the CH_4, with decreasing concentration in the bottom waters: 9 m = 170 ± 13 µM vs. 18 m = 140 ± 11 µM. However, the N_2O concentration showed similar trend as the CH_4, with increasing concentration towards the bottom. Although, no significant differences were seen. The euphotic depth was 13 m depth (at 10:45), while no differences of the turbidity was seen within the profile.

When comparing the CH_4 results between the months, the concentration throughout the water columns shows similar trend of higher concentrations in the bottom waters compared to in the surface waters. While in the bottom waters at the depth of 22 m, August and September provided distinctively higher results than in June. Regarding the $\delta^{13}C_{CH4}$ in June, the trend differs between the months. In June, the sample at 9 m depth (within the thermocline) was lighter than the other samples in the profile. In August, the heaviest composition was found in the surface water, while the profile in September was similar to the ones from B1, with the lightest composition in the surface water. Trends distinguished for the CO_2 concentration and for the N_2O concentration were lower concentrations of CO_2 towards the bottom in August and September and higher concentration of N_2O towards the bottom in all three months. September showed the lowest values of CO_2 at 9-22 m, while June showed the highest at 22 m. The only difference seen between the months for N_2O is at 0 m where June is higher than August.

3.1.3 Surface water: Julaftons Fyr & chamber sites

The results of the CH_4, CO_2 and N_2O concentration as well as of $\delta^{13}C_{CH4}$ of the surface water at Julaftons Fyr, chamber 1 and chamber 2 are presented in figure 8 and table 4.

The results from Julaftons Fyr of the CH_4 concentration showed significant higher values in August and September compared to in June. The results from the isotope analysis of the sample obtained in June could unfortunately not be used due to analytical error. Though, the $\delta^{13}C_{CH4}$ was lighter in August than in September with values of -60.0 ± 0.4‰ and -57.2 ± 0.4‰, respectively. The CO_2 concentrations was significantly higher in June than in September. No differences were seen between the months for the N_2O concentration.

In the surface water at the chambers, it is seen that the CH_4 concentration significantly differed between the months, but with similar trends for the chambers: highest in August and lowest in September. Though, chamber 1 showed generally higher values than chamber 2 in each month. The $\delta^{13}C_{CH4}$ results shows that chamber 1 in August was heavier compared to June and September. The opposite trend is seen at chamber 2, where August composition is lighter compared to June and September. When comparing the results between the chambers,

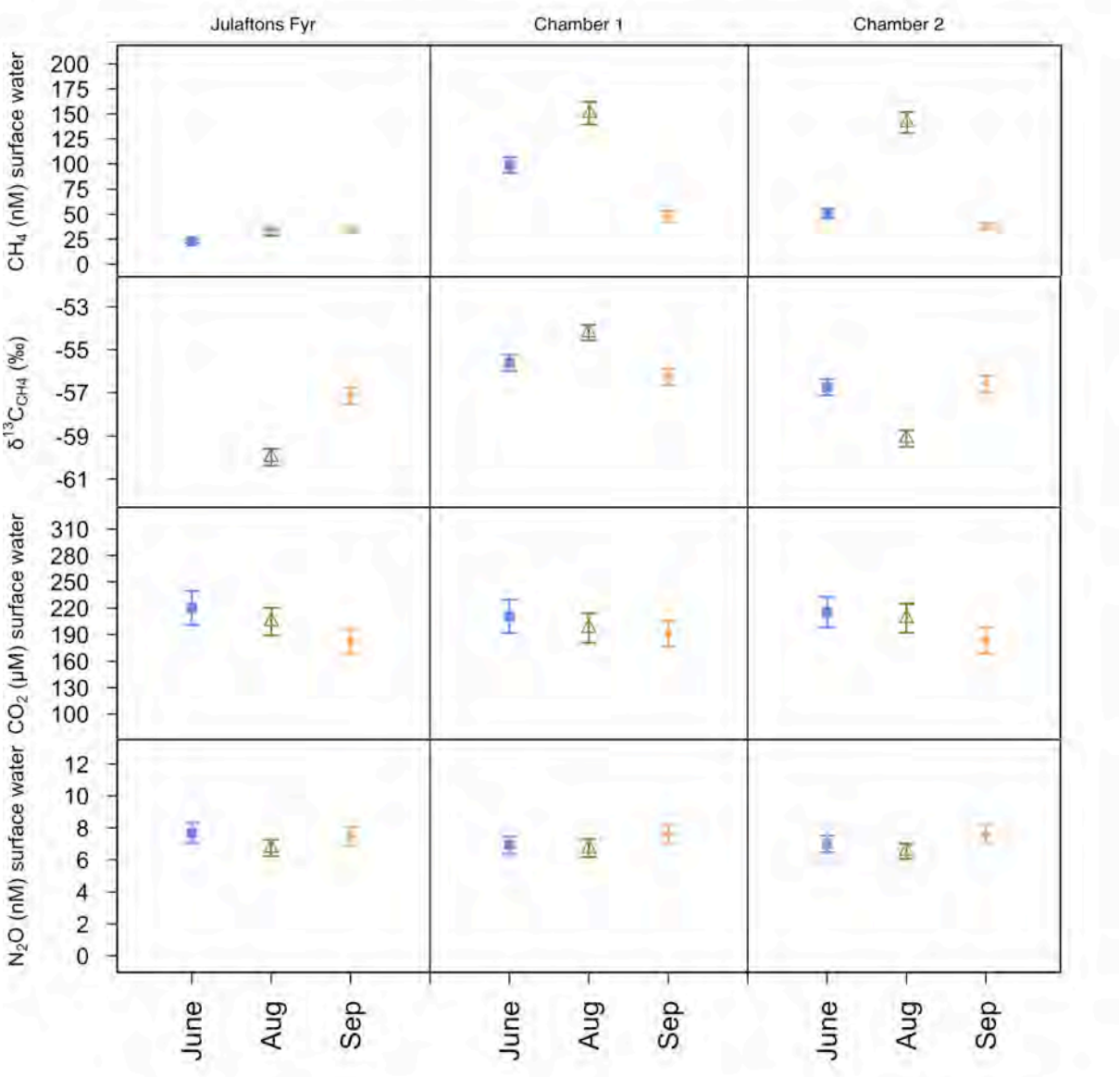

Figure 8. Results from the concentration and isotope analysis from the surface waters at Julaftons Fyr, chamber 1 and at chamber 2. Shared x-axis for all graphs. a) CH_4 concentration (nM) with error bars (standard deviation), b) CO_2 concentration (µM) with error bars (standard deviation), c) N_2O concentration (nM) with error bars (standard deviation), d) isotope composition of $\delta^{13}C_{CH4}$ vs. VPDB (‰) with error bars (standard deviation).

Table 4. Results from the surface waters at Julaftons Fyr, chamber 1 and chamber 2 in J = June, A = August and S = September for CH_4, $\delta^{13}C_{CH4}$, CO_2 and N_2O (average ± standard deviation). In the comment column: D = duplicate samples, T = triplicate samples, X = analytical error during isotope analysis.

Site	*CH_4 (nM) (aver. ± stand. dev.)*	*$\delta^{13}C_{CH4}$ (‰) (aver. ± stand. dev.)*	*CO_2 (µM) (aver. ± stand. dev.)*	*N_2O (nM) (aver. ± stand. dev.)*	*Comments*
Julaftons Fyr	J: 23 ± 1.7	-	J: 220 ± 19	J: 7.7 ± 0.6	D, X
	A: 32 ± 3.4	A: -60.0 ± 0.4	A: 210 ± 15	A: 6.7 ± 0.5	T
	S: 35 ± 2.9	S: -57.2± 0.4	S: 180 ± 14	S: 7.5 ± 0.6	T
Chamber 1	J: 99 ± 7.8	J: -55.6 ± 0.4	J: 210 ± 19	J: 6.9 ± 0.6	D
	A: 151 ± 11	A: -54.2 ± 0.4	A: 200 ± 17	A: 6.7 ± 0.6	T
	S: 48 ± 5.4	S: -56.3 ± 0.4	S: 190 ± 15	S: 7.6 ± 0.6	T
Chamber 2	J: 50 ± 5.0	J: -56.7 ± 0.4	J: 220 ± 17	J: 7.0 ± 0.5	D
	A: 141 ± 11	A: -59.1 ± 0.4	A: 210 ± 17	A: 6.5 ± 0.5	T
	S: 38 ± 3.0	S: -56.6 ± 0.4	S: 180 ± 15	S: 7.7 ± 0.6	T

it is seen that both the composition in June and August were heavier at chamber 1 than at chamber 2. No differences were seen in September. At chamber 1, no differences are seen for CO_2 or N_2O nor for CO_2 at chamber 2. Though at chamber 1, August concentration of N_2O was lower than in September.

3.2 Incubation experiment

The results from the concentration and isotope analysis of the dark incubation samples collected with the Niskin bottle from B1 and Fifångsdjupet in June are presented in figure 9. It was realised that the method for the incubation experiments obtained with a plankton net provided uncertainties in the results. More information regarding the method and results are therefore presented in Appendix 1. In figure 9 below, comparable values from B1 and Fifångsdjupet in June (figure 6 & 7 June = 0 m, minimum and maximum of the error bars) are shown as dashed lines. From the two-sided paired t-test, no significant change in the isotope composition in the experiment samples were seen. Though CH_4, CO_2 and N_2O decreased during the 5 weeks of incubation (CI = 95%). The amount of decrease

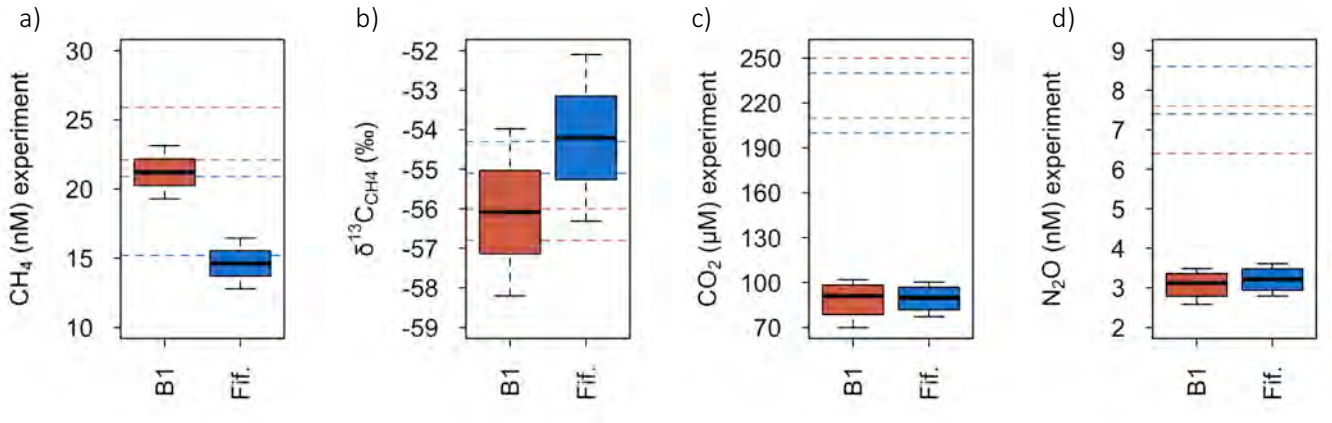

Figure 9. Results from the concentration and isotope analysis of the dark experiment samples from June with 5 weeks incubation. Fif. = Fifångsdjupet. The dashed lines represent the minimum and maximum value of each parameter from the original profile samples at 0 m depth at B1 and Fifångsdjupet from the same month (shown with matching colour scheme). a) CH_4 concentration (nM), b) isotope composition of $\delta^{13}C_{CH4}$ vs. VPDB (‰), c) CO_2 concentration (µM), d) N_2O concentration (nM). Note that none of the y-axes start at zero.

was similar for both sites when observing the total change compared to the original samples (table 5). Further results from the t-tests are found in Appendix 1.

Table 5. The results from the two-sided paired t-test of the change of CH_4, $\delta^{13}C_{CH4}$, CO_2 and N_2O in the dark experiment samples from B1 and Fifångsdjupet in June (5 weeks incubation) with CI = 95%. Negative values show a decrease.

Site	*CH_4 change (nM)*	*$\delta^{13}C_{CH4}$ change (‰)*	*CO_2 change (µM)*	*N_2O change (nM)*
B1	-2.68 ± 0.04	-0.3 ± 4.3	-138 ± 27	-4.1 ± 0.8
Fifångs-djupet	-3.7 ± 0.3	-0.5 ± 4.3	-127 ± 31	-4.7 ± 0.9

3.3 Water-air-fluxes

The results of the water-air-fluxes of CH_4 and of CO_2 measured by the LGR and from the manual flux chambers are presented in the sub chapters below. Though, only some of the measurements of CO_2 and none of the measurement of N_2O provided a statistically significant flux during the days of measurement in the manual flux chamber. These results are therefore not presented in following figures, but provided in Appendix 4: figure A4.1. More specific information regarding parameters (time, air temperature, weather conditions etc) during the air sampling at the chamber sites are presented in Appendix 4: table A4.1 - A4.3, and with graphs of the concentration results (ppm day^{-1} at the chambers and from the LGR measurements, figure A4.2 - A4.3). Further details regarding the parameters during the LGR measurements are presented in Appendix 3.

3.3.1 Methane water-air-fluxes & isotope composition

The CH_4 water-air fluxes from the manual flux chambers and from the LGR are presented in figure 10 and table 6 and the $\delta^{13}C_{CH4}$ of the air samples from the chambers in figure 11. All fluxes are positive, i.e., indicating a flux of methane from water to air. The fluxes were generally higher at the shallower sites in June and August (Julaftons Fyr, Askö and chamber sites). Referring to the figure 10 below, both chambers can be used for trend analyses as well as the LGR results at B1, with the highest fluxes occurred in August of 1.3 mg m^{-2} day^{-1} at B1, 5.0 ± 0.4 mg m^{-2} day^{-1} at chamber 1 and 4.2 ± 0.4 mg m^{-2} day^{-1} at chamber 2. By comparing the results between chamber 1 and 2 it is seen that the fluxes at chamber 1 (chamber located towards open waters) were generally higher than chamber 2, though still showing similar trend in fluxes. There were two different measurements made for each chamber in June where the first measurements (Mon - Tues) were higher than the second (Wedn - Thurs) for both chambers. The second measurements showed similar amount of fluxes as in September for both chambers. When comparing the LGR measurement at Askö in June with the chamber measurements it is seen that it was similar result as chamber 1 in June,

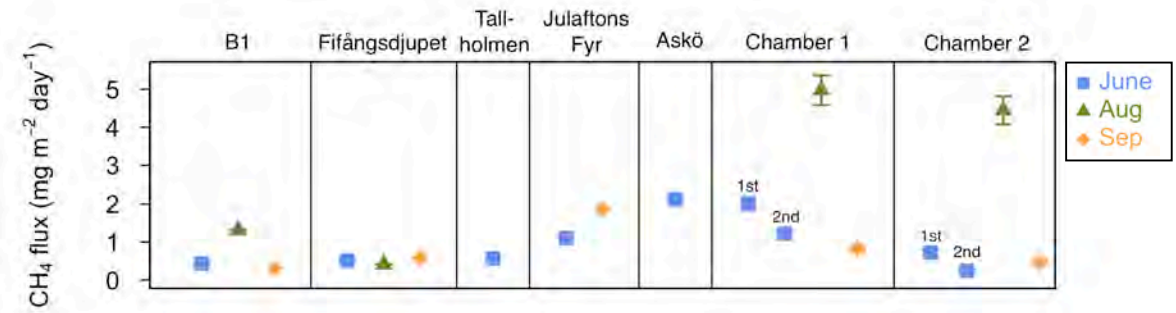

Figure 10. The CH_4 water-air-flux (mg m^{-2} day^{-1}) measured by the LGR (B1, Fifångsdjupet, Tallholmen, Julaftons Fyr, Askö) and with the manual flux chambers (chamber 1 & 2). The CI = 95% of the LGR results and the standard deviations of the chamber results are presented. Two measurement occasions were performed in June at the chamber sites, noted as the 1st measurement (Mon-Tues) and 2nd measurement (Wedn- Thurs).

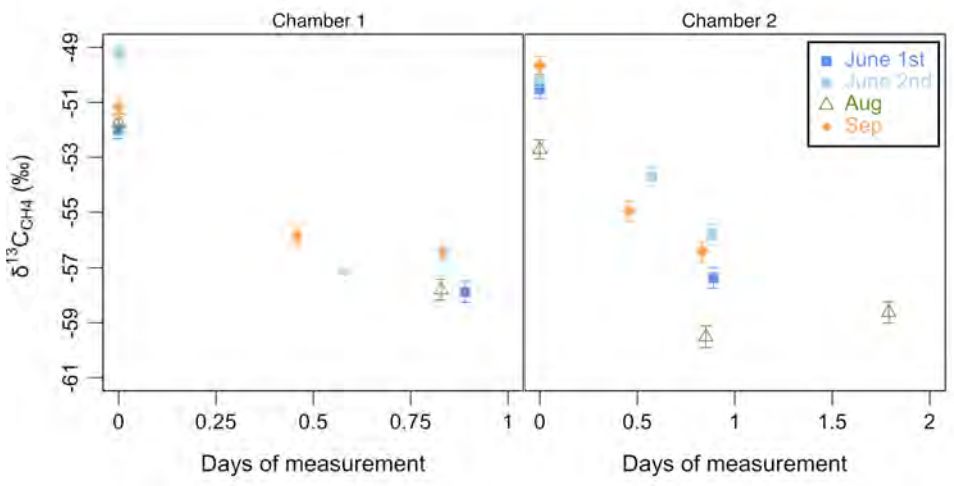

Figure 11. Isotope composition of $\delta^{13}C_{CH4}$ vs. VPDB (‰) with error bars (standard deviation) of the air samples from each day of sample collecting. June 1st = the first measurement (Mon-Tues), June 2nd = the second measurement (Wedn- Thurs).

even though the measurement of the LGR was conducted in the vicinity of chamber 2.
The fluxes at Fifångsdjupet and Julaftons Fyr were higher in September than in June, in contrast to the other sites. The fluxes in June were 0.51 mg m^{-2} day^{-1} at Fifångsdjupet and 1.1 mg m^{-2} day^{-1} at Julaftons Fyr. The measurement at Tallholmen in June provided also similar results as Fifångsdjupet: 0.57 mg m^{-2} day^{-1}.

The $\delta^{13}C_{CH4}$ of the air samples from the chambers showed the same trend for all measurements, where the isotope composition became lighter with time. The atmospheric starting values were in the range of -52.0 ± 0.3‰ to -49.2 ± 0.3‰ at chamber 1 and of -52.7 ± 0.3‰ to -49.7 ± 0.3‰ at chamber 2. The only measurement showing a deviating trend is chamber 2 in August, where the isotope composition at day 2 is heavier (-58.6 ± 0.4‰) than at day 1 (-59.5 ± 0.4‰). This could be an indication of leakage from the chamber (Appendix 5: 5.4).

3.3.2 Carbon dioxide water-air-fluxes

The results from the CO_2 water-air-fluxes varies between the sites where both positive and negative fluxes are seen in figure 12 and table 6. A common factor for B1 and Fifångsdjupet is that negative fluxes occurred at both sites in June and August. The fluxes in August were evidently more negative than in June with -1500

Figure 12. The CO_2 water-air-flux (mg m^{-2} day^{-1}) measured by the LGR (B1, Fifångsdjupet, Julaftons Fyr, Askö) and with the manual flux chambers (chamber 2). The CI = 95% of the LGR results and the standard deviations of the chamber results are presented. Two measurement occasions were performed in June at chamber2, noted as the 1st measurement (Mon-Tues) and 2nd measurement (Wedn- Thurs).

Table 6. Results from the CH_4 and CO_2 water-air-fluxes measured by the LGR and at the chamber sites in J = June, A = August and S = September (LGR results: average ± CI = 95%, chamber results: average ± standard deviation). In the comment column: 1 = 1 day measurement time in the manual flux chambers, 2 = 2 days measurement time in the manual flux chambers, X = no significant flux of CO_2.

Site	*CH_4 flux (mg m^{-2} day^{-1}) (aver. ± stand. dev.)*	*CO_2 flux (mg m^{-2} day^{-1}) (aver. ± stand. dev.)*	*Comments*
B1	J: 0.46 ± 0.02 A: 1.3 ± 0.007 S: 0.31 ± 0.002	J: -170 ± 6 A: -1500 ± 7 S: -130 ± 1	LGR
Fifångsdjupet	J: 0.51 ± 0.03 A: 0.40 ± 0.004 S: 0.57 ± 0.002	J: -220 ± 18 A: -1100 ± 7.4 S: 280 ± 2	LGR
Tallholmen	J: 0.57 ± 0.0005	-	LGR, X
Julaftons Fyr	J: 1.1 ± 0.005 S: 1.9 ± 0.008	J: 590 ± 5 S: 640 ± 3	LGR
Askö	J: 2.1 ± 0.01	J: -490 ± 3	LGR
Chamber 1	J 1^{st}: 2.0 ± 0.6 J 2^{nd}: 1.2 ± 0.3 A: 5.0 ± 0.4 S: 0.83 ± 0.07	- - - -	1 1, X 1, X 2, X
Chamber 2	J 1^{st}: 0.72 ± 0.1 J 2^{nd}: 0.25 ± 0.03 A: 4.5 ± 0.3 S: 0.46 ± 0.1	J 1^{st}: 13 ± 9 J 2^{nd}: -16 ± 14 A: 61 ± 15 -	1, X 2, X 2 2, X

mg m^{-2} day^{-1} and with -1100 mg m^{-2} day^{-1}, respectively. Compared to the other sites, high positive fluxes are seen at Julaftons Fyr for both June and September; 590 mg m^{-2} day^{-1} and mg m^{-2} day^{-1}, respectively. The LGR results from Askö in June differs distinctively from the results of the chambers. The flux of the LGR was -500 mg m^{-2} day^{-1} in contrast to chamber 2 with 13 mg m^{-2} day^{-1}.

3.4 Atmospheric transects

The transects of atmospheric CH_4 from June, August and September are displayed in figure 13. The results in June and August showed similar results, with the exception of the generally higher concentrations at Julaftons Fyr in June (~ 1.89 ppm). This trend is seen neither in August nor in September. Otherwise, the atmospheric CH_4 concentrations at the area of Fifångsdjupet were generally lower (~ 1.87 ppm) than closer the south-western coastline of Askö and with increasing concentration towards the station (~ 1.88 - 1.89 ppm). The results in September is believed to be skewed in accuracy, since the concentration range was generally higher (1.91 - 1.93). The suspicion is that the LGR was in need for calibration, which was not possible during the Askö visit. No other data (fluxes, water concentration) supports the high atmospheric September concentrations. Though when observing the general trend, it is noted that the day when the transect between Fifångsdjupet - Askö was measured (15/9) showed lower concentrations (~ 1.91 - 1.92 ppm) than at the day of the B1 - Askö-transect (14/9, ~ 1.92 - 1.93). Similar wind conditions were observed for both days (Appendix 3).

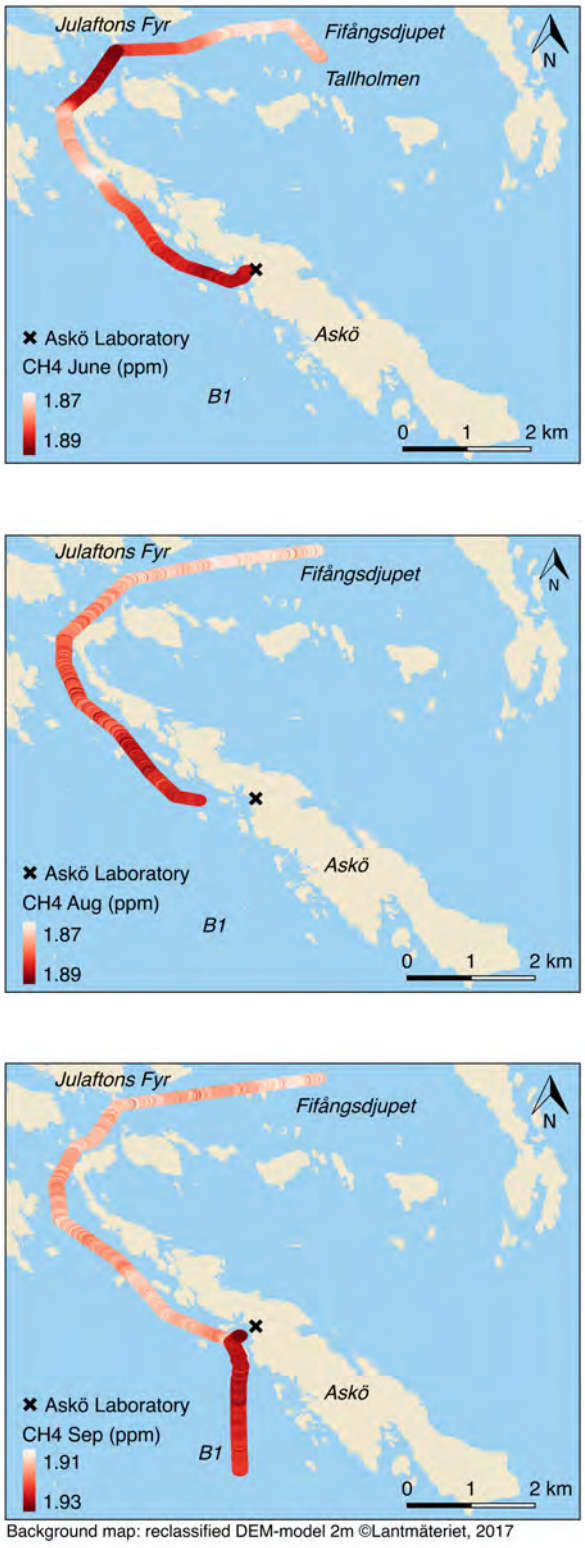

Figure 13. Atmospheric transects of CH_4 concentration (ppm) in a) June (range 1.87 - 1.89 ppm), b) August (range 1.87 - 1.89 ppm) and c) September (1.91 - 1.93 ppm). Note that the concentration range differ in September to the other months and cannot be compared by the colour scheme.

3.5 Qualitative analysis of phytoplankton genera in the water

The qualitative analysis of dominating phytoplankton genera in the water samples are presented in table 7 - 9 and common genera are shown in figure 14. The dominating genus (noted "++++" in the tables) in each month at all sites besides at Fifångsdjupet in August were the cyanobacteria *Aphanizomenon spp.*, which were also accompanied by the cyanobacteria *Skeletonema spp*. in September at B1. At Fifångsdjupet in August, the dominating genus was found to be the ciliate *Tintinnid spp.*, which is a zooplankton. This genus was included anyway due to its high presence. It was also present in the water from Askö experiment area in August and in the September sample from Fifångsdjupet. Other general common genera found was the cyanobacteria *Lyngbya spp*. and *Dolichospermum spp*. Also, *Nodularia spp*. (cyanobacteria) and *Chaetoceros spp*. (diatom) were found in each sample, but with low presence. No accumulation of algae was seen at the water surface in August during sampling, but chlorophyll data (µg/L) from were highest during this month (Appendix 3).

When comparing the number of genera found in each month it is seen that there was higher variation among the genera found in June. Cyanobacteria was the dominating type of phytoplankton in August, where less diatom genera were compared to in June.

Table 7. The results from the qualitative microscope analysis of dominating phytoplankton genus/genera (++++) from the Askö experiment area in June. The "+"-signs shows the relative amount of each phytoplankton genera occurring in the samples.

June	*Askö experiment area*	*Type of phytoplankton*	*Presence*
	Aphanizomenon spp.	Cyanobacteria	++++
	Lyngbya spp.	Cyanobacteria	+++
	Dolichospermum spp.	Cyanobacteria	++
	Chaetoceros spp.	Diatom	++
	Nodularia spp.	Cyanobacteria	++
	Skeletonema spp.	Diatom	+
	Fragilaria spp.	Diatom	+
	Melosira spp.	Diatom	+
	Navicula spp.	Diatom	+
	Stephanodiscus spp.	Diatom	+
	Thalassoira spp.	Diatom	+

Table 8. The results from the qualitative microscope analysis of dominating phytoplankton genus/genera (++++) from the Askö experiment area and Fifångsdjupet in August. The "+"-signs shows the relative amount of each phytoplankton genera occurring in the samples.

Aug	*Askö experiment area*	*Type of phytoplankton*	*Fifångsdjupet*	*Type of phytoplankton*	*Presence*
	Aphanizomenon spp.	Cyanobacteria	*Tintinnid spp.*	Ciliate (zooplankton)	++++
	Lyngbya spp.	Cyanobacteria	*Dolichospermum spp.*	Cyanobacteria	+++
	Tintinnid spp.	Ciliate (zooplankton)	-	-	+++
	Dolichospermum spp.	Cyanobacteria	-	-	+++
	Nodularia spp.	Cyanobacteria	*Nodularia spp.*	Cyanobacteria	++
	Chaetoceros spp.	Diatom	*Chaetoceros spp.*	Diatom	+
	-	-	*Navicula spp.*	Diatom	+
	-	-	*Fragilaria spp.*	Diatom	+

Table 9. The results from the qualitative microscope analysis of dominating phytoplankton genus/genera (++++) from B1 and Fifångsdjupet in September. The "+"-signs shows the relative amount of each phytoplankton genera occurring in the samples.

Sep	*B1*	*Type of phytoplankton*	*Fifångsdjupet*	*Type of phytoplankton*	*Presence*
	Skeletonema spp.	Diatom	*Aphanizomenon spp.*	Cyanobacteria	++++
	Aphanizomenon spp.	Cyanobacteria	-	-	++++
	Lyngbya spp.	Cyanobacteria	*Lyngbya spp.*	Cyanobacteria	++
	Chaetoceros spp.	Diatom	*Dolichospermum spp.*	Cyanobacteria	+
	Dinophysis spp.	Diatom	*Tintinnid spp.*	Ciliate (zooplankton)	+
	Fragilaria spp.	Diatom	*Chaetoceros spp.*	Diatom	+
	Stephanodiscus spp.	Diatom	*Nodularia spp.*	Cyanobacteria	+
	Nodularia spp.	Cyanobacteria	*Skeletonema spp.*	Diatom	+

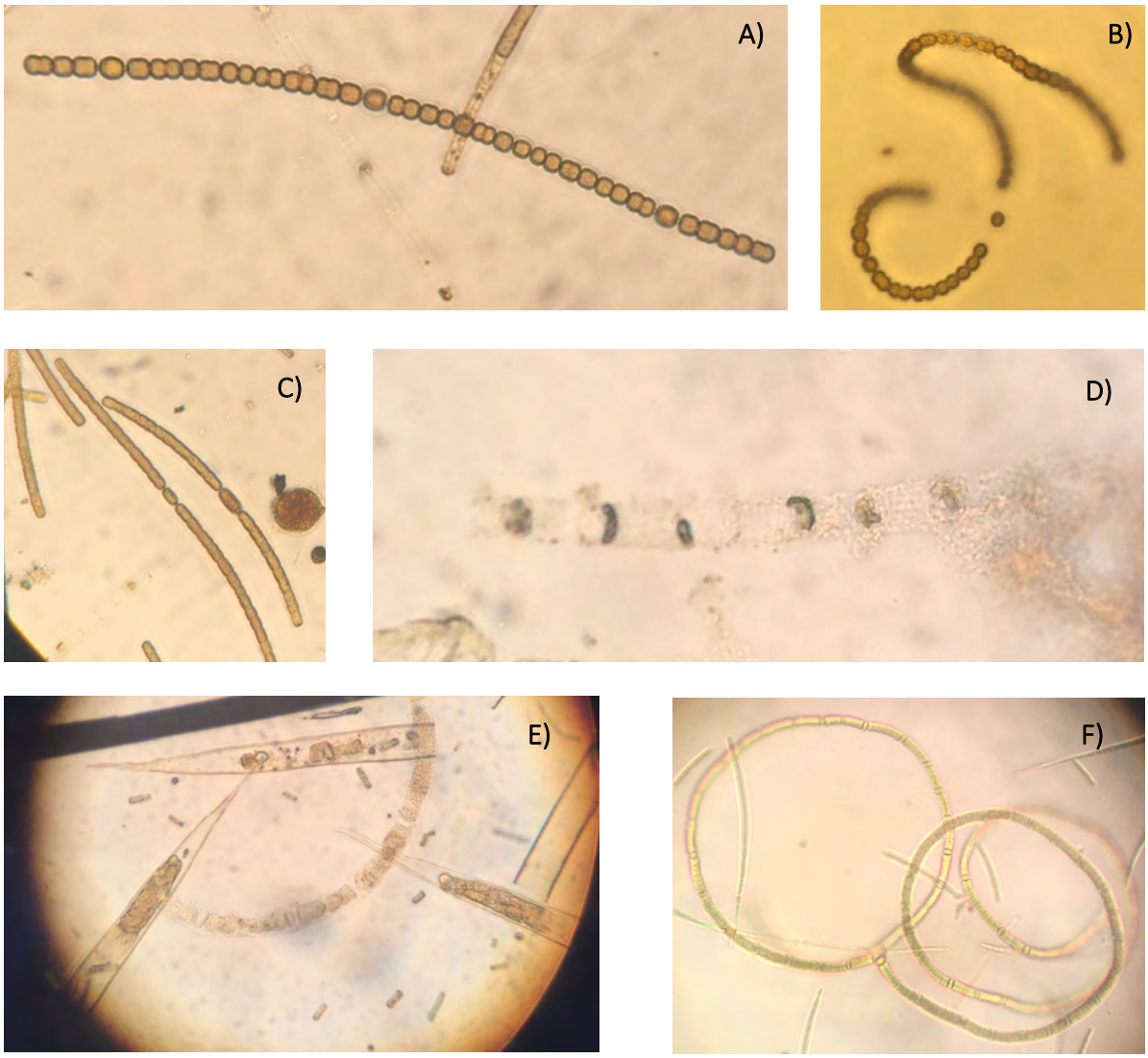

Figure 14. Common phytoplankton genera occurring in the water samples. All images are photographed from the 400x enlargement of the microscope. A & B) *Dolichospermum spp.* (cyanobacteria) C) *Aphanizomenon spp.* (cyanobacteria) D) *Skeletomena spp.* (diatom) E) Three *Tintinnid spp.* (ciliate) and *Nodularia spp.* (cyanobacteria) in the middle, F) *Nodularia spp.*

4. Discussion

What is found in some of the data in this report are seemingly interesting results that are not in line with what a conventional model of a water profile would predict. But before addressing those findings, it is discussed about the results that are in line with what would be predicted. Usually, a water column profile during summer time would be predicted to have stratifications in the profile from the thermocline and the halocline. This would provide distinct changes in dissolved gas concentrations and isotope compositions in the profile (Axell, 1998). In surface waters with high concentrations of gases with respect to the atmosphere, there would be positive water-air-fluxes with dissolved gases emitting from the water. Measured water-air-fluxes of CH_4 in the Baltic Sea have shown values of 0.16-1.9 mg m^{-2} day^{-1} (Bange et al., 1994). Similar values have also been measured in the area around Askö (Brüchert et al., unpublished data). Most of the results presented in this report are in line with these predictions: stratifications in the water column prevented mixing of gases and CH_4 water-air-fluxes generally around 0.5-2 mg m^{-2} day^{-1} (even though fluxes up to 5 mg m^{-2} day^{-1} was measured as well). The methane measurements in the atmospheric transects were all close to the regional atmospheric values of ~ 1.89 ppm (Dlugokencky, 2017), except the concentrations in September showing higher values. As mentioned in the results, the September data may be skewed and have to be corrected by post-calibration of the LGR instrument. The $\delta^{13}C_{CH4}$ values of the atmosphere measured at the chamber sites were ^{13}C-depleted when comparing to the average atmospheric composition of methane of -47.5‰ (Morimoto et al., 2017; Nisbet et al., 2016). However, the concentrations of CH_4 of the atmosphere samples was near a concentration limit of which the GC-IRMS provided more ^{13}C-depleted results than the true values, as shown in tests performed by the laboratory staff. This could have skewed the results, giving generally lighter values.

Considering the results of CO_2, the dissolved CO_2 in the water is a part of the carbonate system, that is dependent on the pH of the water (Schulz, 2006). The CO_2 results are therefore not easy to further interpret without data of the pH. In some of the months, the surface water concentrations were higher than in the bottom water, while in others it were the opposite. Also, the CO_2 fluxes differed between the months and sites, where some were negative and some positive. There are no straightforward explanations for this result, but one can assume that at the measurements sites with negative fluxes the photosynthesis rates were higher. The measured N_2O concentrations are similar to previous measured values (C. Olsson, unpubl. data). No significant fluxes of N_2O was measured, which complies with the fact that the surface concentrations were close to the saturation concentration of N_2O (~7 nM from Sarmiento and Gruber, 2006). Regarding the findings of dominating phytoplankton genera in the surface waters, these were in line with genera usually occurring during summer time in the research area (Stal et al., 2003; Wasmund and Uhlig, 2003). Also, a report from SMHI (2017) that summarised phytoplankton genera occurring near the study site showed presence of similar genera as found here.

Further on to the more interesting findings that are not in line with what would be predicted in a conventional model. What would be predicted is a sediment source of methane that diffuses upwards though the water column. Under these circumstances, it would be expected less amount of CH_4 as well as more ^{13}C-enriched CH_4 in the surface water than in the bottom waters (Schneider von Deimling et al., 2011). This is due to CH_4 oxidation during the ascent in the water column that decreases the concentration and enriches the CH_4 with ^{13}C (Whiticar, 1999). Also, stratifications in the water prevent mixing of the dissolved gas within the water column. The CH_4 in the surface water would also be in equilibrium with the atmosphere, which would provide similar isotope values in the water as in the atmosphere (Knox et al., 1992). A conventional model would also predict an O_2 concentration profile with decreasing concentrations below

the thermocline. That would be due to stratifications in the water, due to less amount of photosynthesis in deeper waters and due to respiration of organic matter using the O_2 in the water (Axell, 1998). However, what is seen in the water profiles at B1 and Fifångsdjupet do not correspond to these predictions. At both sites, it was more enriched $\delta^{13}C_{CH4}$ values in the bottom waters than in the surface waters, with exception at Fifångsdjupet in August. The $\delta^{13}C_{CH4}$ values in the surface waters were more ^{13}C-depleted compared to the atmospheric composition and with concentrations > 700% larger than the saturation concentration (Sarmiento and Gruber, 2006). Also, a CH_4 concentration maxima was seen within the thermocline at B1 in June. From these results, it is assumed that the CH_4 in the surface water above the thermocline would have to have other CH_4 sources besides a vertical transport of diffused gas from the sediment. Regarding the O_2 concentration, the values at B1 in June and August and at Fifångsdjupet in June decreased in the middle of the water column, within or below the thermocline to then further increase below. It is assumed that lateral water input could have occurred, providing the higher O_2 concentrations in the bottom water compared to in the middle of the water columns. These findings have led to three hypotheses, where the first discusses a lateral water input and the two latter discusses other CH_4 sources than diffused gas from the sediment:

- Hypothesis 1) assumption of a lateral input of bottom waters that provided the relative high concentrations of O_2 in the bottom waters. It is discussed whether a possible water input could have affected the $\delta^{13}C_{CH4}$ values in the bottom water as well.

- Hypothesis 2) it is proposed that ebullition bubbles containing ^{13}C-depleted CH_4 reaches up to the mixed layer in the water column. If dissolving in the mixed layer, the $\delta^{13}C_{CH4}$ values of the bubbles mix with the composition of the gas in the water. It is suggested to happen *in situ* at Fifångsdjupet, while ebullition could occur in shallower coastal waters with water currents transporting the ^{13}C-depleted CH_4 out to B1.

- Hypothesis 3) suggestion of a CH_4 production in the photic of the surface water zone at the chamber sites and at B1.

These hypothesises are further elaborated and tested in various ways in the sub-chapters below.

4.1 Hypothesis 1: lateral input of isotopically heavy bottom waters

Hypothesis 1 considers a lateral input of bottom water that effected the O_2 concentration and possibly the isotope composition. The decreased values of O_2 in the middle of the water columns at B1 in June and August and at Fifångsdjupet in June contradicts a predicted O_2 profile. The profiles of the $\delta^{13}C_{CH4}$ values in all months at B1 and in June and September at Fifångsdjupet also contradicts a predicted profile. It could be assumed that lateral input of water effected the profile of the O_2 concentration: either with input of less oxygenated water in the middle of the water column or with higher oxygenated water in the bottom waters. If proceeding with the latter, it could be argued that the water transported laterally into the areas could contain ^{13}C-enriched CH_4. That could provide an explanation for the heavy isotope composition seen in the bottom waters in the months mentioned above. Stratification in the water column prevented mixing with the surface water and thereby providing distinct changes in isotope compositions.

If focusing more on Fifångsdjupet, a conventional profile of $\delta^{13}C_{CH4}$ values was seen in August. It can be assumed that the lateral water input ceased from June into August as well as that the water stratification became weaker, as seen in the results. This could have provided an increased vertical upward transport of diffused CH_4 from the sediment. Supposing that the diffusing CH_4 was more ^{13}C-

depleted then the bottom water, then the isotope composition would become lighter, as also seen in the profile in August. When considering the results from September, no indications of lateral water input were seen in the O_2 data. However, the $\delta^{13}C_{CH4}$ values were yet again more ^{13}C-enriched in the bottom water. If remaining on this hypothesis, the explanation for this result could be that the strong stratification from the thermocline in September inhibited the vertical transport of CH_4 that was allowed in August. When the gas in the bottom water was oxidised, the $\delta^{13}C_{CH4}$ values became heavier and leading to the profile as seen in September.

Regarding the site at B1, the possible lateral input would have ceased into September since the O_2 data showed a conventional profile in that month. However, no indications of a vertical upward transport as a single source of CH_4 to the surface water were inferred in September. The $\delta^{13}C_{CH4}$ values remained more enriched in the bottom water compared to the surface water. It is suggested to be due to the same reason as for Fifångsdjupet: inhibition from a strong stratification of the water and oxidation of CH_4 in the bottom water.

To test if this hypothesis of a lateral input of isotopically heavy bottom water is valid, one would need data of water current directions during the summer of 2017 and of the isotope composition of the diffusing CH_4 from the sediment at Fifångsdjupet. Unfortunately, none of this data have been found and further conclusions cannot be currently made. But assuming that this hypothesis is a valid explanation for these results, the question still remains regarding the source(s) of the CH_4 in the surface waters. The CH_4 concentration increased at B1 from June into August and also at Fifångsdjupet from June into September. Consequently, there must have been other sources contributing to the CH_4 in the surface water to sustain the concentration increase. Further hypotheses of CH_4 sources are therefore examined below.

4.2 Hypothesis 2: methane ebullition

4.2.1 Ebullition in situ at Fifångsdjupet

The second hypothesis to explain the isotope composition in the water column at Fifångsdjupet considers gas ebullition in the area at Tallholmen, as referred to in the introduction. Approximately 600 gas-seepage sites have been identified in the unpublished data (E. Weidner, unpubl. data). One explanation for the results of the $\delta^{13}C_{CH4}$ values could be that bubbles containing CH_4 from seepage sites in the sediment are transported into the mixed layer above the thermocline without being dissolved or oxidised during the ascent. If the bubbles are trapped and then dissolved in the mixed layer, the original isotope composition would be preserved. This could provide the dissolved CH_4 in the surface water a lighter composition than in bottom waters where the CH_4 already has been oxidised. This is illustrated in figure 16. In a study by Schneider von Deimling et al. (2011), the authors concluded that bubbles are able to be transported to the mixed layer. By modelling, they estimated that < 4% of the bubbles from ebullition sites in the North Sea (depth ~ 70 m) reached the mixed layer.

To further investigate the ebullition hypothesis, it was calculated how many bubbles sec^{-1} $seepage\text{-}site^{-1}$ were needed to reach up to the mixed layer between June to August. Details are elaborated in Appendix 5: 5.1. In the calculation, the assumptions were a steady-state of CH_4 concentration between June to August and with ebullition as a single source of CH_4 to the surface water. The observation that < 4% of bubbles from seepage sites reach the mixed layer was assumed to be valid in this scenario. The total seepage flow was calculated as well, meaning the number of bubbles sec^{-1} $site^{-1}$ needed to seep from each site to result in 4% reaching the mixed layer. Various bubbles sizes were used in the calculation, to provide a range of flow needed to occur. The results are presented in table 10.

Table 10. Results from the calculation of number of bubbles sec^{-1} seepage-$site^{-1}$ needed to reach the mixed layer at the Fifångsdjupet area between June - Aug.

Bubble diameter (mm)	*Bubbles reaching the mixed layer (bubbles sec^{-1} $site^{-1}$)*	*Total seep flow (bubbles sec^{-1} $site^{-1}$)*
2	9	225
3	3	75
4	1	25
5	0.6	15
6	0.4	10

The results show that the total seepage flow from the gas-seepage sites at the Fifångsdjupet area is needed to be between 10 - 225 bubbles sec^{-1} $site^{-1}$ whereby 0.4 - 9 bubbles sec^{-1} $site^{-1}$ from this flow are needed to reach up to the mixed layer. The total seep flow provides a flux of approximately 10^{-4} moles sec^{-1} $site^{-1}$ from the sediment. With logical reasoning, the result for the 2 mm bubble size with 225 bubbles sec^{-1} $site^{-1}$ is seemingly a high number. However, the results are credible when comparing to the study by Schneider von Deimling et al. (2011). They found a total ebullition flux from 550 sites of 1.2 moles of CH_4 $year^{-1}$ with average bubble diameters of 4.5 mm. This is equivalent to a flux of 7 * 10^{-5} moles sec^{-1} $site^{-1}$, which is not too different from what was calculated here. An *in situ* ebullition source of CH_4 to the surface water at this site is therefore supported by these results. Though, geophysical acoustic data would be needed to provide further information of bubbles sizes and seepage flow at the ebullition sites.

To expand this hypothesis to B1, where no seepage sites have been noted (as to knowledge of the author at the time of writing), information regarding the availability of CH_4 in the gas phase in the sediment is needed. A study by Sawicka and Brüchert (2017) shows that the CH_4 concentration in the top 5 cm sediment at the sites B1 and H6 (located in Himmerfjärden estuary north of Fifångsdjupet: 58°04'08"N, 17°40'63"E) did not exceed the CH_4 saturation concentration in their measurements. In this regard, no bubbles would be able to escape from the sediment into the water column. This is also observed in Thang et al. (2013) at the site H2 (east of Fifångsdjupet: 58°56"04'N' 17°43"81'E). In that study, the concentration of CH_4 in the top 20 cm of sediment cores did not either exceed the saturation concentration. With these studies in mind, an *in situ* ebullition source of CH_4 into the mixed layer at B1 is not supported. The ebullition hypothesis is therefore further elaborated considering this site.

4.2.2 Ebullition at shallower areas with lateral input of surface waters to B1

The elaboration of the ebullition hypothesis for B1 considers an ebullition source at the shallower areas closer to the coastline, at the chamber sites and Julaftons Fyr. The assumed relative ^{13}C-depleted CH_4 from the ebullition is believed to be laterally transported with

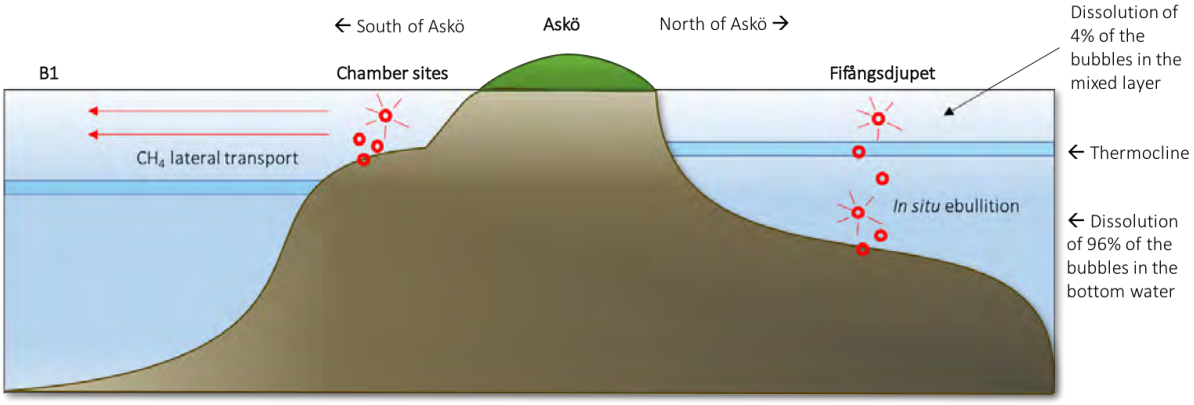

Figure 16. An idealised and simplified illustration of hypothesis 2 (not in scale or with accurate bathymetry). Right: 2.1) *in situ* ebullition contributes to a CH_4 input to the surface water at Fifångsdjupet. 96% of the bubbles are assumed to be dissolved in the bottom waters, while 4% is expected to reach up to the mixed layer. Left: 2.2) ebullition at shallower sites with lateral surface water transport contributes to a CH_4 input to B1.

currents in the surface water from the shallower areas out to the area of B1 (figure 16). The basis for the hypothesis is that similar isotope compositions in the surface water were found at B1 and at the shallower sites. Also, higher CH_4 concentrations were found at the shallower areas compared to at B1, enhancing the idea of a CH_4 source to B1 from the shallower areas. If ebullition takes place at these sites, it would be fair to assume that a larger amount of bubbles would reach the surface water due to the shallow depths (~ 10 – 15 m). It is also considered likely that the bubbles would be transported all the way up to the water surface, which would lead to direct emissions into the atmosphere (Schmale et. al., 2005).

A way to investigate this hypothesis is by searching for indications of direct emissions in the data of the measured water-air-flux at the manual flux chambers. The assumption is that the isotope composition of the possible ebullition bubbles deviates from the composition in the surface water, since no oxidation is believed to have altered the composition of the bubbles. Therefore, if the isotope composition of the water-air-flux (not to be confused with the isotope composition of the air samples of the chambers presented in figure 11) highly deviates from the composition in the surface water, then that could provide indications of direct emissions from an ebullition source. The isotope composition of the fluxes was calculated to test this. The calculation is further elaborated in Appendix 5: 5.2. The calculated values of the fluxes were compared with the isotope composition of the surface water to obtain the difference in isotope composition ($\Delta^{13}C_{CH4}$). For the sake of presentation, the fluxes from the three months of the two chambers were grouped into four groups: group N, D, DN1 and DN2, where "N" refers to that the fluxes occurred during night time and "D" during day time. The fluxes in group N were coupled with the fluxes in group D and also group DN1 coupled with group DN2. This is clarified in table 11.

The results from of the $\Delta^{13}C_{CH4}$ values are presented in figure 17 and table 12. A schematic overview of the results of chamber 2 in September is also presented in figure 18 to provide a better understanding of the grouping of the days and for better distinguishing of the various parameters used in the flux calculation in Appendix 5.

Table 11. Table of the grouped fluxes. The column "Sampling" shows between which sampling occasions that the fluxes occurred.

Group	*Sampling*	*Hours between sampling*	*Day/night*
N	1st to 2nd	~ 12	Night
D	2nd to 3rd	~ 12	Day
DN1	1st to 2nd	~ 24	Day & night
DN2	2nd to 3rd	~ 24	Day & night

The result for group DN2 showed a positive $\Delta^{13}C_{CH4}$ value, thus with a flux with heavier isotope composition than the surface water. However, the assumption is that leakage might have occurred during the sampling between the 2nd and 3rd sampling occasion at the chamber in group DN2. That would have mixed the air inside of the chamber with air in the atmosphere, thereby giving the chamber air a heavier isotope composition. That would in return alter the results for the calculation made here. Further examination of a possible leakage is given in Appendix 5: 5.4. The results of the $\Delta^{13}C_{CH4}$ from group DN2 is therefore disregarded in further discussion.

Table 12. Results from the difference in isotope composition $\Delta^{13}C_{CH4}$ (‰) ± standard deviation between the calculated fluxes and the surface water at the chamber sites. Negative values show of more ^{13}C-depleted flux than surface water and vice versa. J 1st = June 1st measurement, J 2nd = June 2nd measurement, A = August, S = September.

Group	*Chamber 1: $\Delta^{13}C_{CH4}$ (‰), min-max*	*Chamber 2: $\Delta^{13}C_{CH4}$ (‰), min-max*
N	J 2nd: -2.7 ± 0.4 S: -0.5 ± 0.4	J 2nd: 0.2 ± 0.4 S: -0.4 ± 0.4
D	J: - S: -0.9 ± 0.4	J 2nd: -2.6 ± 0.4 S: -4.1 ± 0.4
DN1	J 1st: -2.6 ± 0.4 A: -3.8 ± 0.4	J 1st: -1.7 ± 0.4 A: -0.7 ± 0.4
DN2	A: -	A: *0.9 ± 0.4*

In order to draw more solid conclusions on the importance of direct emissions for the fluxes,

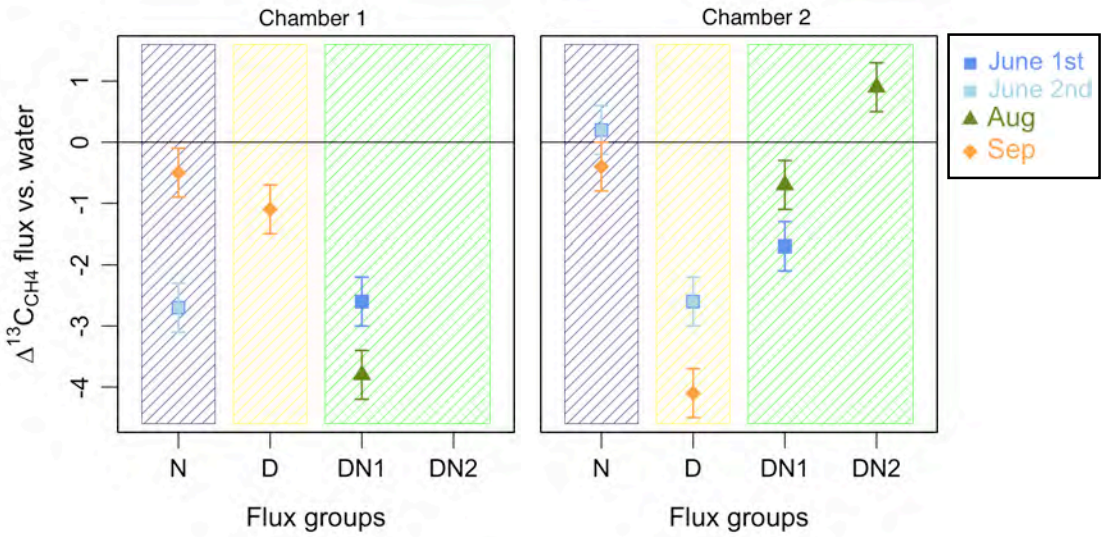

Figure 17. Results from the calculation of the difference in isotope composition $\Delta^{13}C_{CH4}$ vs. VPDB (‰) from the calculated flux composition at the chambers sites compared to the composition of the surface water at the chamber sites for each month. Negative values show of lighter composition of the flux than the water and vice versa. The shaded backgrounds represent the time the fluxes occurred during: dark blue = night time, yellow = day time, green = day & night time. June 1st = the first measurement made in June (Mon - Tues), June 2nd = the second measurement made in June (Wedn - Thurs).

the isotope composition of CH_4 bubbles from the sediment must be measured at the specific sites. It is also important to consider that if the fluxes contain both water-air-fluxes and direct emissions, then the isotope composition will be a mixture of the compositions from two sources. Though, what is interesting to see in the result is that the composition of the fluxes in group N were close to zero (exception of chamber 1: June 2nd: group N), meaning that the fluxes did not differ much from the surface water. Group D and DN1, on the other hand, were all lighter than the surface water as well as generally lighter compared to group N. This could show that the fluxes occurring during day time are lighter than fluxes occurring during

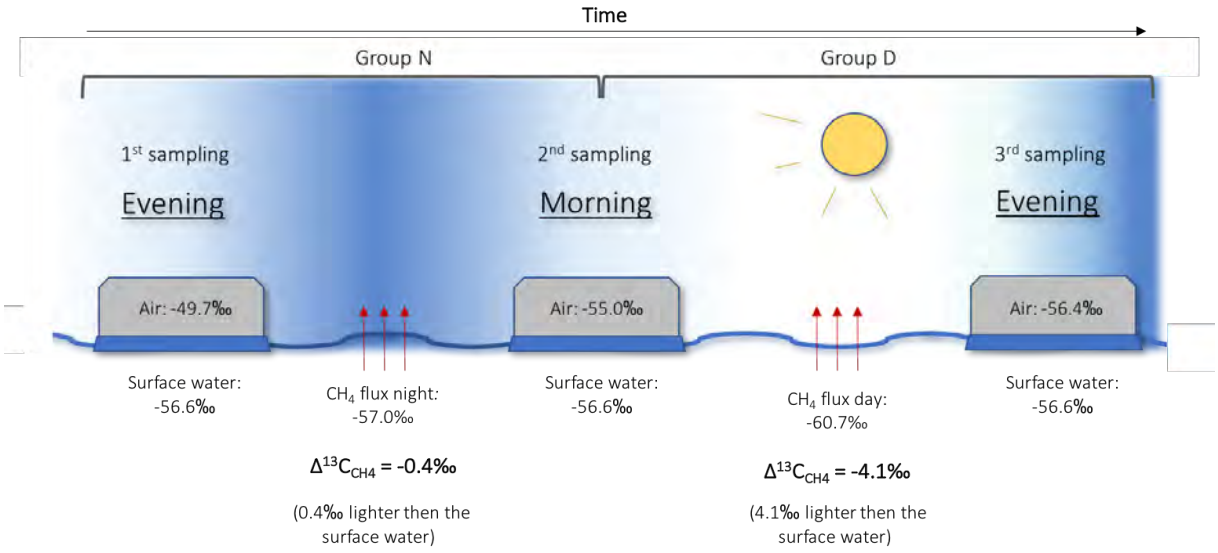

Figure 18. Schematic overview of the parameters used in the equation in Appendix 5: 5.4 as well as the results from chamber 2 in September (figure 17) as an example: $\delta^{13}C_F = CH_4$ flux night, $\delta^{13}C_X$ = air in the chamber at the 1st sampling and $\delta^{13}C_{TOT}$ = air in the chamber in the 2nd sampling. The values presented in the figure are the average results from chamber 2 in September, where the day fluxes (-60.7‰) are lighter than the night fluxes (-57.0‰). Group N: flux between the 1st and 2nd sampling, group D: flux between the 2nd and 3rd sampling. The chamber air becomes lighter with time due to mixing with the ^{13}C-depleted flux.

night time. A reason for this result could be due to variation in wind strength between day and night that could influence the flux, since wind speed has a direct effect on the flux (Wanninkhof et al., 2009). However, no indications of a specific relationship were seen in the amount of flux with day time/night time (Appendix 5: 5.3) and it could be argued that there would therefore not be a relationship with the isotope composition as well. Another reason for the result could be a CH_4 production source in the photic zone during day time influencing the flux isotope composition.

To further verify if there could occur ebullition in the shallower areas, geophysical acoustic data would be needed. To also further verify if there could be lateral transport of CH_4 from the shallower sites to B1, information regarding water currents are necessary. None of these data were possible to obtain within the framework of this work.

4.3 Hypothesis 3: methane production in the oxygenated surface water

From previous discussion, it was apparent that day light presumably had an effect on the isotope composition of the water-air-fluxes at the chamber sites in all three months. This could indicate of a CH_4 production coupled with biological activity occurring under light conditions. This supports the main hypothesis for this report, i.e., that measurable methane production occurs in the oxygenated surface water in the photic zone. This finding does also support the main hypothesis that this production significantly contributes to a CH_4 water-air-flux, since the concentrations at the chamber sites increased in August during the algal bloom. The production pathway in the main hypothesis was believed to be hydrogenotrophic methano-genesis. As mentioned in the introduction, this pathway uses H_2 as a main component which can be produced during nitrogen fixation by cyanobacteria (Bothe et al., 2010) and occurs mostly under light conditions (Hong, 1992). However, it cannot be concluded whether hydrogenotrophic methanogenesis could be the pathway, more data before doing so would be needed.

Considering the results for the dark incubation experiment, no indications of CH_4 production were shown. Though, the CO_2 and N_2O concentrations provided indications of biological activity. If light incubations had been conducted with the same method, it would had been interesting to compare if any differences were seen between the dark and light samples. If higher CH_4 concentrations and/or lighter isotope values had been seen in the light samples, further conclusions could have been made regarding a CH_4 production under light conditions. The conclusions to be drawn for now is that no CH_4 production occurred under dark conditions. However, an indication of CH_4 production in the oxygenated surface water at B1 in June is the concentration maxima of CH_4 within the thermocline. This is in line with what other studies have found regarding methane production in oxygenated surface waters; a production in conjunction with the thermocline (Schneider von Deimling et al., 2011; Tang et al., 2014). In the study by Schneider von Deimling et al. (2011), the authors found methane maxima within the thermocline as well as lighter isotope composition compared to bottom and surface waters. They suggested an *in situ* biological production for their results.

One final indication of methane production in the oxygenated, photic zone is the relationship between the CH_4 and CO_2 water-air-fluxes measured by the LGR at B1 and Askö (in the vicinity of the chamber sites). Graphs of CH_4 versus CO_2 concentrations from the LGR measurements are presented in Appendix 6. A negative linear relationship is seen in all measurements at B1, the measurement at Askö in June and at Fifångsdjupet in August ($r^2 >$ 0.98). Thus, increasing concentrations of CH_4 were seen during decreasing concentrations of CO_2. This could be interpreted as a CH_4 production occurring during uptake of CO_2. The second component in the hydrogenotrophic methano-genesis is CO_2 and this result could be an indication of this pathway. However, both measurements made at Julaftons Fyr and the September measurement at Fifångsdjupet showed the opposite: increasing CO_2 with

increasing CH_4 ($r^2 > 0.98$). This can suggest that there is actually not a true relationship between the gases, but instead that the concentration of both gases changes linearly independently of each other.

4.4 Final comments

One alternative not discussed in this report is methane production in aggregates of phytoplankton. Within these aggregates, anoxic conditions are formed, thus creating an environment in the surface water of which methane production can occur (Grossart et al., 2011). During algal blooms, the conditions of this kind of production would increase due to larger amount of phytoplankton in the water. However, it would be assumed that the production would be higher in dark conditions when photosynthesis is shut off, giving less oxygen in the water. Though, that contradicts what is believed to be found here. One would also consider a higher amount of methane production in the sediment during algal blooms, which could explain the higher concentrations found in August. Due to the larger amount of cyanobacteria decomposing at the seafloor during the blooms, conditions for higher rates of methane production are given.

It should be emphasised the complexity of the subject that is investigated in this report. The dissolved CH_4 in the water is effected by various parameter, changing in both time and space: biological activity, the structure of the water column, wind conditions, temperature, salinity, water currents, fluxes from the sediment as well as to the atmosphere, access to production components and so on. To therefore create a broad understanding of the subject, a lot of parameters are needed to be in consideration.

5. Conclusions

This study has shown that the surface water at the area around Askö have high concentrations of methane and is a source to the atmosphere. It is also shown that the water south of Askö (B1) must have had a CH_4 source not only from a vertical upward transport of CH_4 diffusing from the sediment. A suggestion of another source is CH_4 ebullition from the sediment in the shallower waters at the southern coastline of Askö (chamber sites) with water currents possibly transporting the gas laterally towards the open coastal waters at B1. It is also suggested that a CH_4 production could occur under light conditions in the mixed layer at B1 and around the chamber sites, a production presumably higher during the algal bloom. The latter supports the main hypothesis for this study: a methane production in the oxygenated surface water that significantly contributes to a CH_4 water-air-flux and that increases during the algal bloom.

In the waters of the northern side of Askö in the more enclosed basin at Fifångsdjupet, a vertical upward transport of CH_4 is reasonable as a single source to the surface water in August. However, the amount of transport must had been high enough to sustain the concentration increase seen during the summer. A hypothesis for a second methane source is therefore presented, *in situ* ebullition from the 600 gas seepage sites at the seafloor in the nearby area with bubbles reaching the mixed layer. If ebullition would be the only source of CH_4 to the mixed layer, a total seepage flow to sustain the CH_4 concentration from June into August was estimated to 10 - 225 bubbles sec^{-1} $site^{-1}$ with 4% of these bubbles reaching the mixed layer. In comparison to other studies, these numbers are fairly reasonable. However, to draw any further conclusion regarding ebullition as a source, the flow at the seepage sites at Fifångsdjupet would need to be investigated.

Acknowledgements

First and foremost, I would like to give my greatest gratitude to my supervisors Volker Brüchert at the Department of Geological

Sciences at Stockholm University and Helle Ploug at the Department of Marine Sciences at the University of Gothenburg. Your knowledge, guidance and enthusiasm have made this bachelor thesis possible and have encouraged me to explore what for me was a quite unknown topic. I am especially thankful to Volker for all the vast amount of e-mails and long meetings that always provided me with insights. I am grateful for all the help and support that the staff at Askö Laboratory provided me during my visits to the station and out on the water with the research vessel R/V Limanda, in both sunny and rainy weather conditions. I am also grateful to my loving Toni Axelsson, who without any question gave his last week of vacation to the task of being my field assistance and has also supported me throughout the entire process. And Jonas Fredriksson, who helped me in the field in September and joined me in the struggle of rowing a boat for 90 minutes during a creaking sound from the oars. I would also like to thank Heike Siegmund at the Stable Isotope Laboratory (SIL) at Stockholm University, who with enthusiasm supported me during the isotope analysis. I also want to thank Joachim Jansen, Lena Kautsky and other staff at Stockholm University that in various ways have helped me. Lastly, I would like to thank friends and family that have shown interest and joy for this bachelor thesis during the process.

References

Angelis, M.A.D., Lee, C., 1995. Methane production during zooplankton grazing on marine phytoplankton. Oceanogr. Lit. Rev. 7, 539.

Axell, L.B., 1998. On the variability of Baltic Sea deepwater mixing. J. Geophys. Res. Oceans 103, 21667–21682. https://doi.org/10.1029/98JC01714

Bange, H.W., Bartell, U.H., Rapsomanikis, S., Andreae, M.O., 1994. Methane in the Baltic and North Seas and a reassessment of the marine emissions of methane. Glob. Biogeochem. Cycles 8, 465–480. https://doi.org/10.1029/94GB02181

Berg, A., Lindblad, P., Svensson, B.H., 2014. Cyanobacteria as a source of hydrogen for methane formation. World J. Microbiol. Biotechnol. 30, 539–545. doi:10.1007/s11274-013-1463-5

Björck, S., 1995. A review of the history of the Baltic Sea, 13.0-8.0 ka BP. Quat. Int. 27, 19–40. https://doi.org/10.1016/1040-6182(94)00057-C

Bothe, H., Schmitz, O., Yates, M.G., Newton, W.E., 2010. Nitrogen Fixation and Hydrogen Metabolism in Cyanobacteria. Microbiol. Mol. Biol. Rev. 74, 529–551. https://doi.org/10.1128/MMBR.00033-10

Bousquet, P., Ciais, P., Miller, J.B., Dlugokencky, E.J., Hauglustaine, D.A., Prigent, C., Van der Werf, G.R., Peylin, P., Brunke, E.-G., Carouge, C., Langenfelds, R.L., Lathière, J., Papa, F., Ramonet, M., Schmidt, M., Steele, L.P., Tyler, S.C., White, J., 2006. Contribution of anthropogenic and natural sources to atmospheric methane variability. Nature 443, 439–443. https://doi.org/10.1038/nature05132

Carstensen, J., Andersen, J.H., Gustafsson, B.G., Conley, D.J., 2014. Deoxygenation of the Baltic Sea during the last century. Proc. Natl. Acad. Sci. 111, 5628–5633. https://doi.org/10.1073/pnas.1323156111

Clark, I., 2015. Groundwater Geochemistry and Isotopes. Taylor & Francis Group.

Codispoti, L.A., Brandes, J.A., Christensen, J.P., Devol, A.H., Naqvi, S.W.A., Paerl, H.W., Yoshinari, T., 2001. The oceanic fixed nitrogen and nitrous oxide budgets: Moving targets as we enter the anthropocene? Sci. Mar. 65, 85–105.

Conrad, R., 2005. Quantification of methanogenic pathways using stable carbon isotopic signatures: a review and a proposal. Org. Geochem., Stable isotope applications in methane cycle studies 36, 739–752. https://doi.org/10.1016/j.orggeochem.2004.09.006

Damm, E., Helmke, E., Thoms, S., Schauer, U., Nöthig, E., Bakker, K., Kiene, R.P. 2010. Methane production in aerobic oligotrophic surface water in the central Arctic Ocean. Biogeosciences 7:1099–1108

Deppenmeier, U., Müller, V., Gottschalk, G., 1996. Pathways of energy conservation in methanogenic archaea. Arch. Microbiol. 165, 149–163. https://doi.org/10.1007/BF01692856

Dlugokencky, E.J., P.M. Lang, A.M. Crotwell, J.W. Mund, M.J. Crotwell, and K.W. Thoning (2017), Atmospheric Methane Dry Air Mole Fractions from the NOAA ESRL Carbon Cycle Cooperative Global Air Sampling Network, 1983-2016, Version: 2017-07-28, Path: ftp://aftp.cmdl.noaa.gov/data/trace_gases/ch4/flask/surface/

Ferry, J.G., 1993a. Methanogenesis: Ecology, Physiology, Biochemistry & Genetics, Chapman & Hall Microbiology Series. Springer.

Ferry, J.G., 1993b. Fermentation of Acetate. SpringerLink 304–334. https://doi.org/10.1007/978-1-4615-2391-8_7

Gelwicks, J.T., Risatti, J.B., Hayes, J.M., 1994. Carbon isotope effects associated with aceticlastic methanogenesis. Appl. Environ. Microbiol. 60, 467–472.

Grossart, H.-P., Frindte, K., Dziallas, C., Eckert, W., Tang, K.W., 2011. Microbial methane production in oxygenated water column of an oligotrophic lake. Proc. Natl. Acad. Sci. 108, 19657–19661. https://doi.org/10.1073/pnas.1110716108

Gülzow, W., Rehder, G., Schneider v. Deimling, J., Seifert, T., Tóth, Z., 2013. One year of continuous measurements constraining methane emissions from the Baltic Sea to the atmosphere using a ship of opportunity. Biogeosciences 10, 81–99. https://doi.org/10.5194/bg-10-81-2013

Hansson, M., 2006. Cyanobakterieblomningar i Östersjön, resultat från satellitövervakning 1997-2005. SMHI.

Ho, D.T., Bliven, L.F., Wanninkhof, R., Schlosser, P., 1997. The effect of rain on air-water gas exchange. Tellus B 49, 149–158. https://doi.org/10.1034/j.1600-0889.49.issue2.3.x

Hong, G.-F., 1992. The Nitrogen Fixation and its Research in China, 1st ed. Springer-Verlag Berlin Heidelberg.

IPCC, 2013: *Climate Change 2013: The Physical Science Basis. Contribution of Working Group I to the Fifth Assessment Report of the Intergovernmental Panel on Climate Change* [Stocker, T.F., D. Qin, G.-K. Plattner, M. Tignor, S.K. Allen, J. Boschung, A. Nauels, Y. Xia, V. Bex and P.M. Midgley (eds.)]. Cambridge University Press, Cambridge, United Kingdom and New York, NY, USA, 1535 pp. http://www.climatechange2013.org/images/report/WG1AR5_ALL_FINAL.pdf

Johnson, K.M., Hughes, J.E., Donaghay, P.L., McN. Sieburth, J. 1990. Bottle-Calibration Static Head Space Method for the Determination of Methane Dissolved in Seawater. Analytical Chemistry, vol. 62, no. 21, 2408-2412

Karl, D.M., Beversdorf, L., Björkman, K.M., Church, M.J., Martinez, A., Delong, E.F., 2008. Aerobic production of methane in the sea. Nat. Geosci. 1, 473–478. https://doi.org/10.1038/ngeo234

Karl, D.M., Tilbrook, B.D., 1994. Production and transport of methane in oceanic particulate organic matter. Nature 368, 732–734. https://doi.org/10.1038/368732a0

Klawonn, I., Nahar, N., Walve, J., Andersson, B., Olofsson, M., Svedén, J.B., Littmann, S., Whitehouse, M.J., Kuypers, M.M.M., Ploug, H., 2016. Cell-specific nitrogen- and carbon-fixation of cyanobacteria in a temperate marine system (Baltic Sea). Environ. Microbiol. 18, 4596–4609. https://doi.org/10.1111/1462-2920.13557

Knox, M., Quay, P.D., Wilbur, D., 1992. Kinetic isotopic fractionation during air-water gas transfer of O2, N2, CH4, and H2. J. Geophys. Res. Oceans 97, 20335–20343. https://doi.org/10.1029/92JC00949

Kustmätsystem. 2017. Askö. https://www.smhi.se/kustmatsystem/asko (From the dates given in the tables of the appendices)

Lee, Z., Weidemann, A., Kindle, J., Arnone, R., Carder, K.L., Davis, C., 2007. Euphotic zone depth: Its derivation and implication to ocean-color remote sensing. J. Geophys. Res. Oceans 112, C03009. https://doi.org/10.1029/2006JC003802

Mah, R.A., Ward, D.M., Baresi, L., Glass, T.L., 1977. Biogenesis of Methane. Annu. Rev. Microbiol. 31, 309–341. https://doi.org/10.1146/annurev.mi.31.100177.001521

Morimoto, S., Fujita, R., Aoki, S., Goto, D., Nakazawa, T., 2017. Long-term variations of the mole fraction and carbon isotope ratio of atmospheric methane observed at Ny-Ålesund, Svalbard from 1996 to 2013. Tellus B Chem. Phys. Meteorol. 69, 1380497. https://doi.org/10.1080/16000889.2017.1380497

Nisbet, E.G., Dlugokencky, E.J., Manning, M.R., Lowry, D., Fisher, R.E., France, J.L., Michel, S.E., Miller, J.B., White, J.W.C., Vaughn, B., Bousquet, P., Pyle, J.A., Warwick, N.J., Cain, M., Brownlow, R., Zazzeri, G., Lanoisellé, M., Manning, A.C., Gloor, E., Worthy, D.E.J., Brunke, E.-G., Labuschagne, C., Wolff, E.W., Ganesan, A.L., 2016. Rising atmospheric methane: 2007–2014 growth and isotopic shift. Glob. Biogeochem. Cycles 30, 2016GB005406. https://doi.org/10.1002/2016GB005406

Penger, J., Conrad, R., Blaser, M., 2012. Stable Carbon Isotope Fractionation by Methylotrophic Methanogenic Archaea. Appl. Environ. Microbiol. 78, 7596–7602. https://doi.org/10.1128/AEM.01773-12

Reeburgh, W.S., Heggie, D.T., 1977. Microbial methane consumption reactions and their effect on methane distributions in freshwater and marine environments1. Limnol. Oceanogr. 22, 1–9. https://doi.org/10.4319/lo.1977.22.1.0001

Sarmiento, J., Gruber, N., 2006. Ocean Biogeochemical Dynamics. Princeton University Press, New Jersey.

Sawicka, J.E., Brüchert, V., 2017. Annual variability and regulation of methane and sulfate fluxes in Baltic Sea estuarine sediments. Biogeosciences 14, 325–339. https://doi.org/10.5194/bg-14-325-2017

Schmale, O., Schneider von Deimling, J., Gülzow, W., Nausch, G., Waniek, J.J., Rehder, G., 2010. Distribution of methane in the water column of the Baltic Sea. Geophys. Res. Lett. 37, L12604. https://doi.org/10.1029/2010GL043115

Schneider von Deimling, J., Rehder, G., Greinert, J., McGinnnis, D.F., Boetius, A., Linke, P., 2011. Quantification of seep-related methane gas emissions at Tommeliten, North Sea. Cont. Shelf Res. 31, 867–878. https://doi.org/10.1016/j.csr.2011.02.012

Schmale, O., Greinert, J., Rehder, G., 2005. Methane emission from high-intensity marine gas seeps in the Black Sea into the atmosphere. Geophys.

Res. Lett. 32, L07609. https://doi.org/10.1029/2004GL021138

Schulz, H.D., 2006. Quantification of Early Diagenesis: Dissolved Constituents in Pore Water and Signals in the Solid Phase, in: Marine Geochemistry. Springer, Berlin, Heidelberg, pp. 73–124. https://doi.org/10.1007/3-540-32144-6_3

Scranton, M.I., Brewer, P.G., 1977. Occurrence of methane in the near-surface waters of the western subtropical North-Atlantic. Deep Sea Res. 24, 127–138. https://doi.org/10.1016/0146-6291(77)90548-3

SGU (Geological Survey of Sweden). 2015. *Marine Geology, vector: resolution 1:100 000.* https://maps.slu.se/get (Hämtat 2016-10-22)

SMHI (Swedish Meteorological and Hydrological Institute). 2017. Nyhetsarkiv: Sommarens algblomning var tydligast i norra Östersjön. https://www.smhi.se/nyhetsarkiv/sommarens-algblomning-var-tydligast-i-norra-ostersjon-1.125392 (From 2018-01-03)

Stal, L.J., Albertano, P., Bergman, B., Bröckel, K. von, Gallon, J.R., Hayes, P.K., Sivonen, K., Walsby, A.E., 2003. BASIC: Baltic Sea cyanobacteria. An investigation of the structure and dynamics of water blooms of cyanobacteria in the Baltic Sea—responses to a changing environment. Cont. Shelf Res., European Land-Ocean Interaction 23, 1695–1714. https://doi.org/10.1016/j.csr.2003.06.001

Tang, K.W., McGinnis, D.F., Frindte, K., Brüchert, V., Grossart, H.-P., 2014. Paradox reconsidered: Methane oversaturation in well-oxygenated lake waters. Limnol. Oceanogr. 59, 275–284. https://doi.org/10.4319/lo.2014.59.1.0275

Thang, N.M., Brüchert, V., Formolo, M., Wegener, G., Ginters, L., Jørgensen, B.B., Ferdelman, T.G., 2013. The Impact of Sediment and Carbon Fluxes on the Biogeochemistry of Methane and Sulfur in Littoral Baltic Sea Sediments (Himmerfjärden, Sweden). Estuaries Coasts 36, 98–115. https://doi.org/10.1007/s12237-012-9557-0

Wang, F.K., 2001. Confidence interval for the mean of non-normal data. Qual. Reliab. Eng. Int. 17, 257–267. https://doi.org/10.1002/qre.400

Wanninkhof, R., Asher, W.E., Ho, D.T., Sweeney, C., McGillis, W.R., 2009. Advances in quantifying air-sea gas exchange and environmental forcing. Annu. Rev. Mar. Sci. 1, 213–244. https://doi.org/10.1146/annurev.marine.010908.163742

Wasmund, N., Uhlig, S., 2003. Phytoplankton trends in the Baltic Sea. ICES J. Mar. Sci. 60, 177–186. https://doi.org/10.1016/S1054-3139(02)00280-1

Weiss, R.F., 1974. Carbon dioxide in water and seawater: the solubility of a non-ideal gas. Mar. Chem. 2, 203–215. https://doi.org/10.1016/0304-4203(74)90015-2

Weiss, R.F., Price, B.A., 1980. Nitrous oxide solubility in water and seawater. Mar. Chem. 8, 347–359. https://doi.org/10.1016/0304-4203(80)90024-9

Whiticar, M.J., 1999. Carbon and hydrogen isotope systematics of bacterial formation and oxidation of methane. Chem. Geol. 161, 291–314. https://doi.org/10.1016/S0009-2541(99)00092-3

Whiticar, M.J., Faber, E., Schoell, M., 1986. Biogenic methane formation in marine and freshwater environments: CO2 reduction vs. acetate fermentation—Isotope evidence. Geochim. Cosmochim. Acta 50, 693–709. https://doi.org/10.1016/0016-7037(86)90346-7

Wiesenburg, D.A., Guinasso, N.L. 1979. Equilibrium Solubilities of Methane, Carbon Monoxide, and Hydrogen in Water and Sea Water. Journal of Chemical and Engineering Data, vol. 24, no. 4, 356-360.

Yamamoto, S., Alcauskas, J.B., Crozier, T.E., 1976. Solubility of methane in distilled water and seawater. J. Chem. Eng. Data 21, 78–80. https://doi.org/10.1021/je60068a029

Appendix 1

A1.1. Results two-sided paired t-test of the incubation experiment samples

The results from the two-sided paired t-test performed in R Studio for the incubation experiment presented in figure 9 and table 5 in the results are given below in table A1.1 (B1) and table A1.2 (Fifångsdjupet).

Table A1. Results from the two-sided paired t-test from B1. Null hypothesis that the mean difference is equal to 0. Df = degrees of freedom (n - 1).

	t-value	*Df*	*p-value*	*Mean difference*
CH_4	276.58	2	$1.307 * 10^{-5}$	2.7
$\delta^{13}C_{CH4}$	-0.32172	2	0.7782	-0.32
CO_2	22.267	2	$2.011 * 10^{-3}$	140
N_2O	22.66	2	$1.942 * 10^{-3}$	4.1

Table A2. Results from the two-sided paired t-test from Fifångsdjupet. Null hypothesis that the mean difference is equal to 0. Df = degrees of freedom (n - 1).

	t-value	*Df*	*p-value*	*Mean difference*
CH_4	59.477	2	$2.826 * 10^{-4}$	3.7
$\delta^{13}C_{CH4}$	-0.53092	2	0.6485	-0.53
CO_2	17.656	2	$3.192 * 10^{-3}$	130
N_2O	23.422	2	$1.818 * 10^{-3}$	4.7

A1.2 Incubation experiment: method

The experiment was conducted differently in June compared to in August and September, where figure A1.2 demonstrates the details. To collect water samples for the incubation experiment, the Niskin bottle was used for two of the three experiments in June, to obtain samples containing low amount of phytoplankton (as explained in *2.2 Field methods*). A plankton net (4.1 µm) was used for the other experiments in June at the Aug Askö experiment are, in August at the June Askö experiment area and in September at B1 and Fifångsdjupet. Only dark incubation experiments were conducted in June, while in August and September both light and dark incubations were made to distinguish effects of light and dark conditions. In the latter, control samples were also made with filtered water, where all phytoplankton were removed.

When collecting samples with the plankton net, the water was firstly poured into a 2 L glass bottle when being out in the field. The water for the unfiltered incubation experiment was poured through a funnel into glass bottles of 110 mL and fitted with a butyl stopper and aluminium seal. The filtered samples were streamed into the bottles through a syringe with a 0.45 µm filter attached to it. This removed all the phytoplankton, while bacteria and archaea remained. The samples obtained with the plankton net

were incubated for 24 hours. The June samples from the Niskin bottle were stored in a cooling room of 15°C for 5 weeks, while samples from August and September were stored at the surface water below the deck at the station at the Askö Laboratory. This was made to simulate similar environmental conditions as the conditions of where the organisms where obtained from. To end the incubation, 1 mL of $ZnCl_2$ (zinc chloride, 50% concentration) was added.

The results from the plankton net method were not presented in the results of this report since gas was lost during the sampling and transferring process. No samples with starting values of concentration and isotope composition were made for this method, i.e., samples that were not incubated. No reference values were therefore available to compare any changes. However, it was assumed that the filtered samples were in equilibrium with the atmosphere (concentration CH_4 ~ 2.6 nM, CO_2 ~ 12 µM, N_2O ~ 7 nM (Sarmiento and Gruber, 2006), $\delta^{13}C_{CH4}$ near atmospheric composition around -50‰ to -48‰). The other samples transferred to the glass bottles through a funnel was assumed not being as much equilibrated, but still have lost parts of the gases. Though, no confirmation of this was being able to be made.

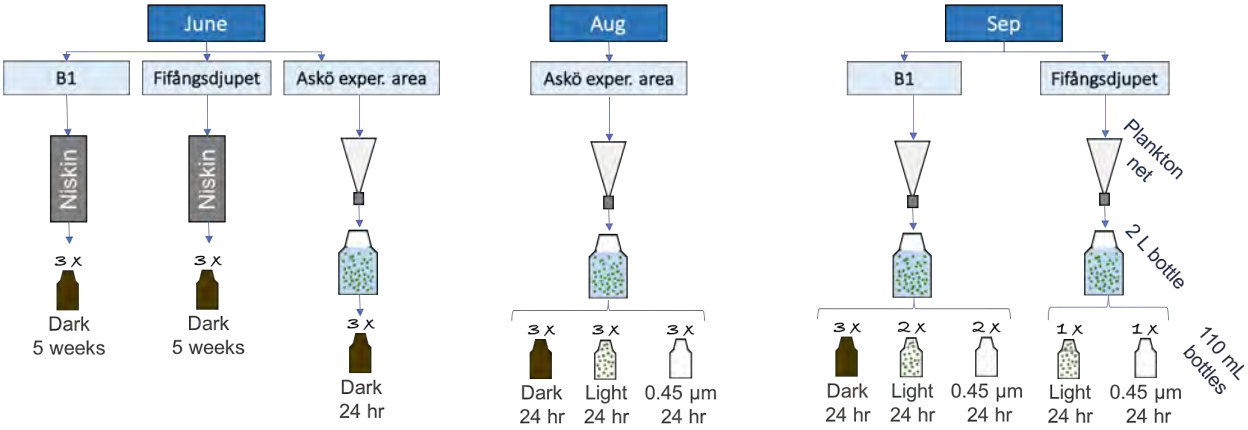

Figure A1.2. A schematic overview of how the incubation experiments were conducted for each occasion, where left = June, middle = August and right = September.

A1.3 Incubation experiment: results

The results from all of the incubation experiments are presented in figure A1.2. None of the analysed parameters in the filtered samples showed of expected values, as mentioned in the method description. The CH_4 and N_2O concentrations were higher, the CO_2 concentration lower and the $\delta^{13}C_{CH4}$ was lighter than expected. When comparing the results between the months for samples obtained with the same method, no distinguishing differences were seen. For the unfiltered samples, the CH_4 concentration were in the same range for both light and dark samples, though, with a slightly higher value in June at Askö experiment area:

- June dark Askö = 14 ± 2.3 nM
- Aug light = 10 ± 1.7 nM
- Aug dark = 12 ± 1.0 nM
- Sep light B1 = 11 ± 1.1 nM
- Sep dark B1 = 11 ± 1.2 nM
- Sep light Fifångsdjupet = 10 ± 0.75 nM

The filtered sample in August were lower in CH_4 concentration than the experiment from Fifångsdjupet in September. However, it was only a small difference:

- Aug = 6.1 ± 0.72 nM
- Sep B1 = 8.1 ± 1.8 nM
- Sep Fifångsdjupet = 10 ± 0.74 nM

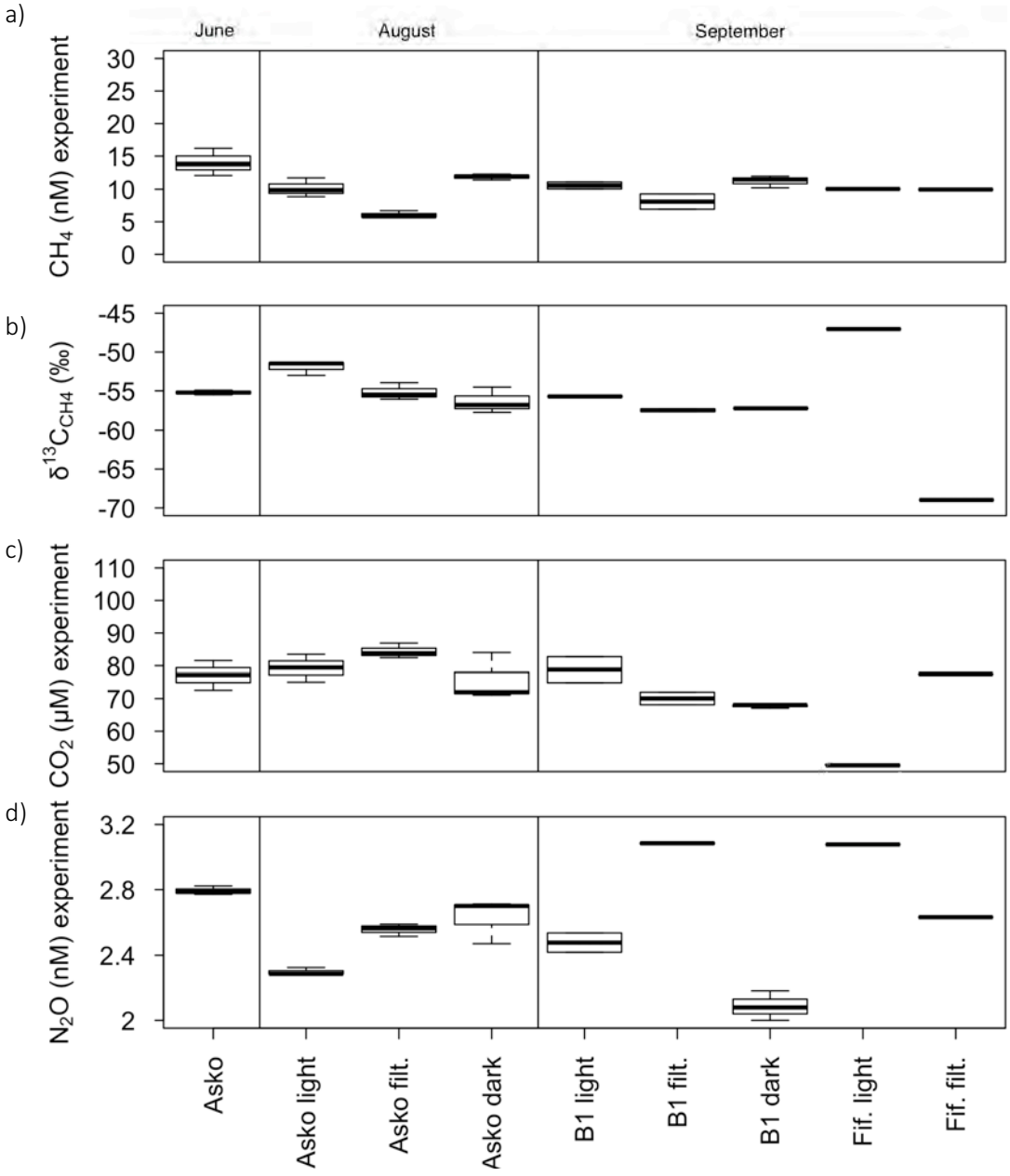

Figure A1.3. Results from the concentration and isotope analysis of the experiment samples from June (left), August (middle) and September (right) that were not presented in the main results-section. Asko=Askö experiment area, Fif.=Fifångsdjupet, filt.=light samples filtered with 0.45 µm filter. a) CH_4 concentration (nM), b) isotope composition of $\delta^{13}C_{CH4}$ vs. VPDB (‰), c) CO_2 concentration (µM), d) N_2O concentration (nM). Note: only single samples were obtained at Fifångsdjupet in September.

The $\delta^{13}C_{CH4}$ values were in the same range for all samples (~ -56‰ to ~ -54‰), with values slightly more depleted than seen in the surface water of the study sites. Exception of this though was at Fifångsdjupet in September, where the unfiltered samples provided value of -47.0 ± 0.3‰ and the filtered sample of -69.0 ± 0.5‰. As well the light experiment in August provided value of -51.9 ± 0.1‰. It must be

mentioned that due to the relative low concentrations of CH_4 in the incubation bottles, the reliability of the results from the GC-IRMS was low. Tests performed by the laboratory staff with known standards show a high standard deviation at the levels of peak areas that these samples showed. This standard deviation is not included in the error bars in the graph. Though after consideration, these results are still presented since the results from the duplicates and triplicates provided results in the same composition range. However, this might have skewed the results at Fifångsdjupet in September, where only single samples were obtained and no comparison of other samples can be made.

All of the samples provided similar results in CO_2 and N_2O concentration with CO_2 range between ~ 70 to ~ 85 µM and N_2O between ~ 2.1 to ~ 2.6 nM. These values were in close range to the June experiment obtained from the Niskin bottle. The only small differences seen were lower CO_2 values in the light September experiment from Fifångsdjupet (50 ± 3.7 µM) as well as higher N_2O concentration in the filtered sample from B1 and in the light Fifångsdjupet experiment in September (3.1 ± 0.2 nM for both).

No further interpretation of the result is made, since no reference samples were obtained and it is not truly known if the water was in equilibrium with the atmosphere as assumed.

Appendix 2

The coefficients used in equation 6 when calculating the Bunsen solubility coefficients for the gases CH_4, CO_2 and N_2O are presented in table A2.

Table A2. Coefficients for the Bunsen solubility coefficient β (moles liter^{-1} atm^{-1}) of the dry mole fraction of the gases CH_4, CO_2 and N_2O.

Gas	*A1*	*A2*	*A3*	*B1*	*B2*	*B3*	*Calculated β (moles L^{-1} atm^{-1})*	*Reference*
CH_4	-68.8862	101.4956	28.7314	-0.076146	0.04397	-0.0068672	0.033461	Wiesenburg and Guinasso (1979)
CO_2	-58.0931	90.5069	22.294	0.027766	-0.025888	0.0050578	0.038187	Weiss (1974)
N_2O	-62.7062	97.3066	24.1406	-0.05842	0.033193	-0.0051313	0.027992	Weiss and Price (1980)

Appendix 3

Table A3.1 - A3.3 below present the information regarding the field conditions during the sampling and measurements at B1, Fifångsdjupet, Tallholmen, Julaftons Fyr and at Askö for each occasion in June, August and September. The chlorophyll data was gathered from the coastal measurement system at B1 (Kustmätsystem, 2017). The remaining data was gathered on the research vessel R/V Limanda.

Table A3.1. Sampling parameters obtained during the water sampling, CTD and LGR measurement at the various sites in June. Temp = temperature, surf. = surface, sal. = salinity, press. = pressure.

Site June	*Date*	*Time*	*Temp. air (°C)*	*Temp. surf. water (°C)*	*Sal. (PSU)*	*Wind: speed (m/s) & direction*	*Air press. (hPa)*	*Chlorophyll (µg/L)*	*Weather*
B1	2017-06-28	09:00	15	12.9	6.3	2.8 – 4.0 (ESE)	1011	0.69	Sunny
Fifångsdjupet	2017-06-28	11:10	15	15.8	6.3	3.5 – 4.5 (ESE)	1012	0.69	- II -
Julaftons Fyr	2017-06-28	13:00	15	-	-	3.6 (SE)	1012	0.69	- II -
Askö (LGR)	2017-06-28	13:45	15	-	-	3.3 – 7.2 (ESE)	1012	-	- II -
June Askö exp. area	2017-06-29	11:00	15	13.8	6.2	9.7 (-)	1007	0.72	- II -

Table A3.2. Sampling parameters obtained during the water sampling, CTD and LGR measurement at the various sites in August. Temp = temperature, surf. = surface, sal. = salinity, press. = pressure.

Site Aug	*Date*	*Time*	*Temp. air (°C)*	*Temp. surf. water (°C)*	*Sal. (PSU)*	*Wind: speed (m/s) & direction*	*Air press. (hPa)*	*Chlorophyll (µg/L)*	*Weather*
Askö (exp. area)	2017-08-02	09:00	20.3	18.5	5.9	2.0 (-)	1009.5	2.7	Sunny
B1	2017-08-03	11:26	17	18.6	6.1	4.5 – 8.0 (S-SSE)	1011	3.0	Sunny & windy
Fifångsdjupet	2017-08-03	13:01	18	18.8	6.2	4.5 – 8.0 (S-SSE)	1010	3.0	- II -
Julaftons Fyr	2017-08-03	13:42	18	-	-	4.5 – 8.0 (S-SSE)	1010	3.0	- II -

Table A3.3. Sampling parameters obtained during the water sampling, CTD and LGR measurement at the various sites in September. Temp = temperature, surf. = surface, sal. = salinity, press. = pressure.

Site Sep	*Date*	*Time*	*Temp. air (°C)*	*Temp. surf. water (°C)*	*Sal. (PSU)*	*Wind: speed (m/s) & direction*	*Air press. (hPa)*	*Chlorophyll (µg/L)*	*Weather*
B1	2017-09-14	14:00	14	14.8	6.3	5.5 – 8.0 (NNW)	985	2.4	Partly rain and cloudy
Fifångsdjupet	2017-09-15	10:45	13	14.9	6.3	5.0 – 6.5 (NW)	997	2.1	Sunny
Julaftons Fyr	2017-09-15	12:10	14	-	-	3.4 – 6.0 (NW)	998	2.1	Sunny

Appendix 4

Table A4.1 - A4.3 below present the information regarding the field conditions during the air and water samplings at the chamber sites for each occasion in June, August and September. The air temperature, wind speed, air pressure and chlorophyll data was gathered from the coastal measurement system at B1 (Kustmätsystem, 2017). The water temperature and salinity were measured by a conductivity meter.

Table A4.1. Sampling parameters obtained during the air and water sampling at the chamber sites in June. Temp = temperature, surf. = surface, sal. = salinity, press. = pressure, x = no sampling made at chamber 1.

June	*Date*	*Time*	*Temp. air (°C)*	*Temp. surf. water (°C)*	*Sal. (PSU)*	*Wind speed (m/s)*	*Air press. (hPa)*	*Chlorophyll (µg/L)*	*Weather*
Monday	2017-06-26	17:38, 17:55	11.6	15.4, 15.1	6.1, 6.1	7.5	997.2	1.3	Sunny (rain earlier during the day)
Tuesday	2017-06-27	15:06, 15:17	11.6	14.6, 14.8	6.1, 6.1	2.6	1007.5	0.82	Sunny
Wednesday	2017-06-28	17:10, 17:30	15.0	14.4, 14.8	6.1, 6.1	5.7	1011.4	0.71	- II -
Thursday morning	2017-06-29	07:09, 07:20	15.0	13.8, 13.6	6.1, 6.2	8.4	1009.3	0.71	- II -
Thursday afternoon	2017-06-29	x, 14.39	15.0	x, 14.8	6.2	10.9	1006.2	0.82	- II -

Table A4.2. Sampling parameters obtained during the air and water sampling at the chamber sites in August. Temp = temperature, surf. = surface, sal. = salinity, press. = pressure.

Aug	*Date*	*Time*	*Temp. air (°C)*	*Temp. surf. water (°C)*	*Sal. (PSU)*	*Wind speed (m/s)*	*Air press. (hPa)*	*Chlorophyll (µg/L)*	*Weather*
Monday	2017-07-31	15:22, 14:55	20.4	19.1, 20.2	5.9, 5.8	4.7	1008.9	3.6	Sunny
Tuesday	2017-08-01	11:15, 11:22	17.5	19.4, 19.2	5.9, 5.8	6.2	1015.3	2.5	Windy, a bit cloudy
Wednesday	2017-08-02	09.43, 09:52	18.5	19.2, 19.4	5.9, 5.9	2.0	1009.4	2.5	Sunny, a little bit of rain
Thursday	2017-08-03	08:08, 08:20	16.0	19.2, 19.0	5.9, 5.9	4.3	1011.5	2.1	Sunny (rain during the wedn.-thurs.-night)
Friday	2017-08-04	07:59, 08:07	16.1	19.3, 18.8	5.9, 5.8	6.4	998.2	2.7	Sunny & windy

Table A4.3. Sampling parameters obtained during the air and water sampling at the chamber sites in September. Temp = temperature, surf. = surface, sal. = salinity, press. = pressure.

Sep	*Date*	*Time*	*Temp. air (°C)*	*Temp. surf. water (°C)*	*Sal. (PSU)*	*Wind speed (m/s)*	*Air press. (hPa)*	*Chlorophyll (µg/L)*	*Weather*
Thursday	2017-09-14	19:00, 19:30	12.5	14.9, 14.8	6.2, 6.2	3.5	989.7	2.1	Rain on and off during the day
Friday morning	2017-09.15	09:03, 09:10	13.2	14.4, 14.4	6.2, 6.2	3.0	996.5	1.9	Sunny
Friday afternoon	2017-09.15	14:44, 14:55	15.5	14.9, 14.8	6.2, 6.2	1.4	999.4	2.2	- II -

The results in ppm day^{-1} from of the analysis of CH_4, CO_2 and N_2O of all of the air samples obtained from the chamber sites are presented figure A4.1, even the ones not used in the water-air-flux calculations. If no significant difference was seen between the samples or if the starting value of the sample was skewed (e.g. the first sample of CO_2 in June 1st with ~ 600 ppm in the atmosphere), no calculation was made. The measurement results of ppm day^{-1} from the LGR measurements from each site of CH_4 are presented in figure A4.2 and of CO_2 in figure A4.3.

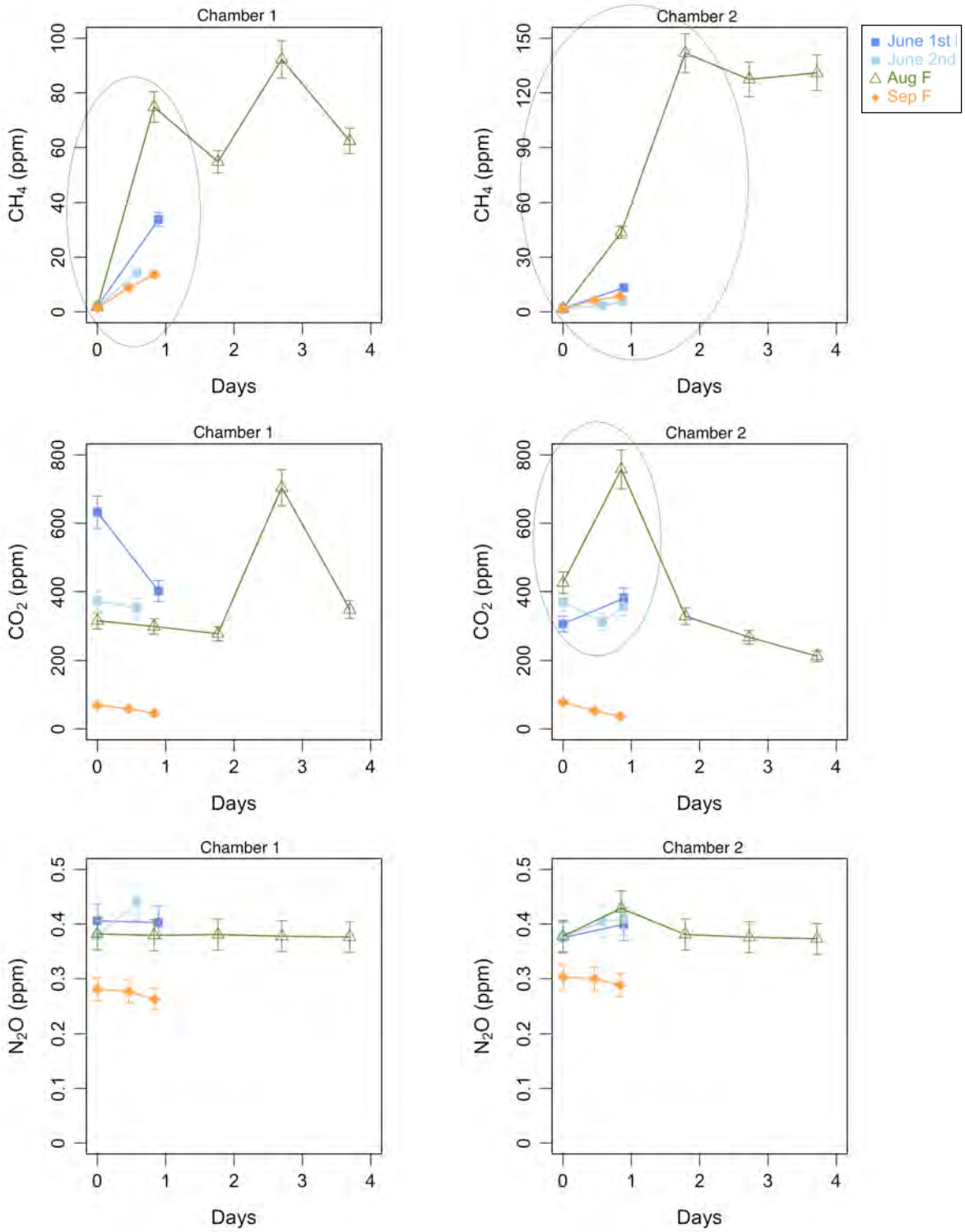

Figure A4.1. The results from the air sample analysis of CH_4 (top), CO_2 (middle) and N_2O (bottom) from each sample obtained at chamber 1 (left) and chamber 2 (right) in June, August and September. The circles show which samples that were used in the calculation of the fluxes. However, the third sample of CO_2 in June 2nd (light blue) was not included in the flux calculation. No significant fluxes were measured of N_2O at all. Shared legend for all graphs.

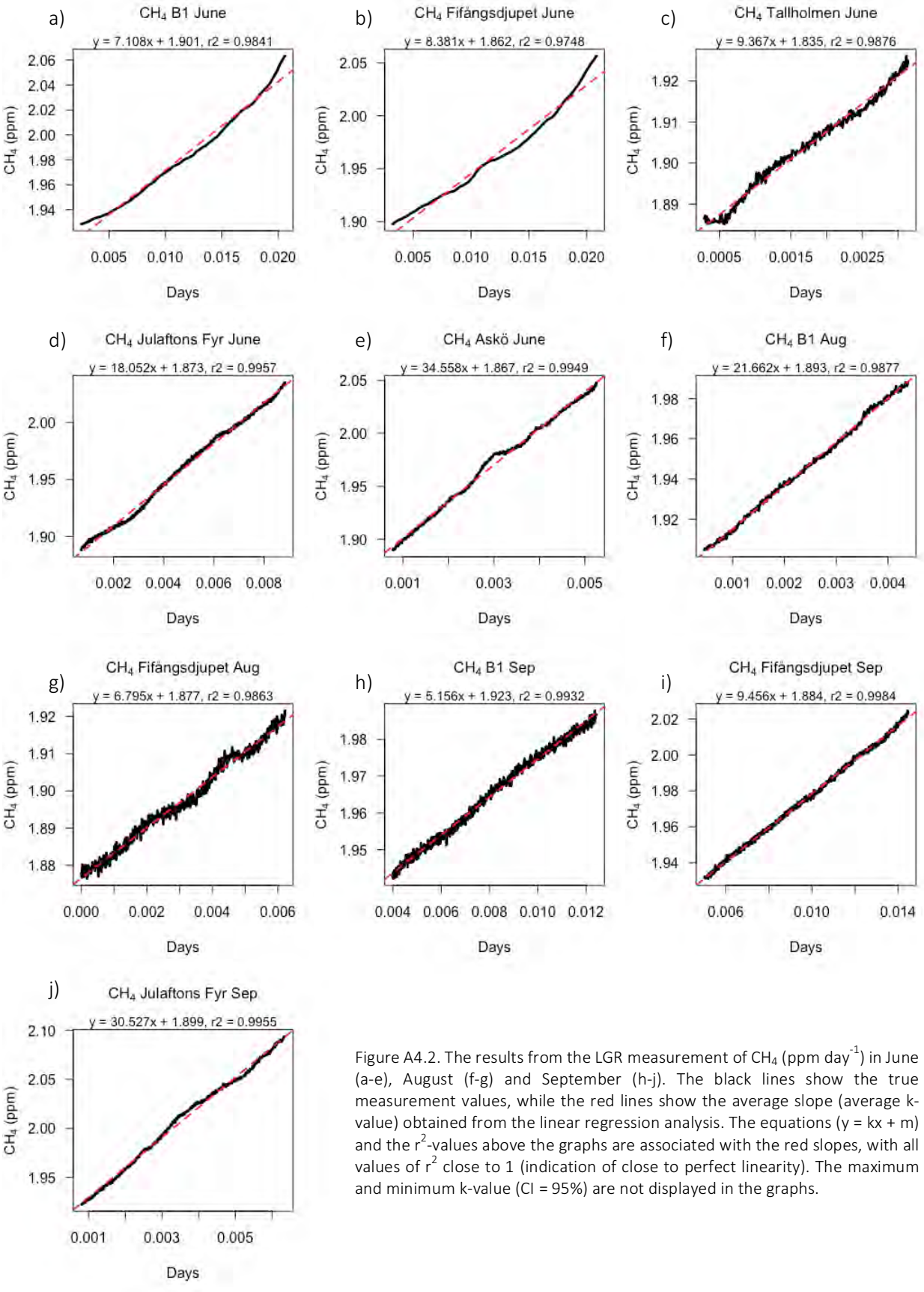

Figure A4.2. The results from the LGR measurement of CH_4 (ppm day^{-1}) in June (a-e), August (f-g) and September (h-j). The black lines show the true measurement values, while the red lines show the average slope (average k-value) obtained from the linear regression analysis. The equations (y = kx + m) and the r^2-values above the graphs are associated with the red slopes, with all values of r^2 close to 1 (indication of close to perfect linearity). The maximum and minimum k-value (CI = 95%) are not displayed in the graphs.

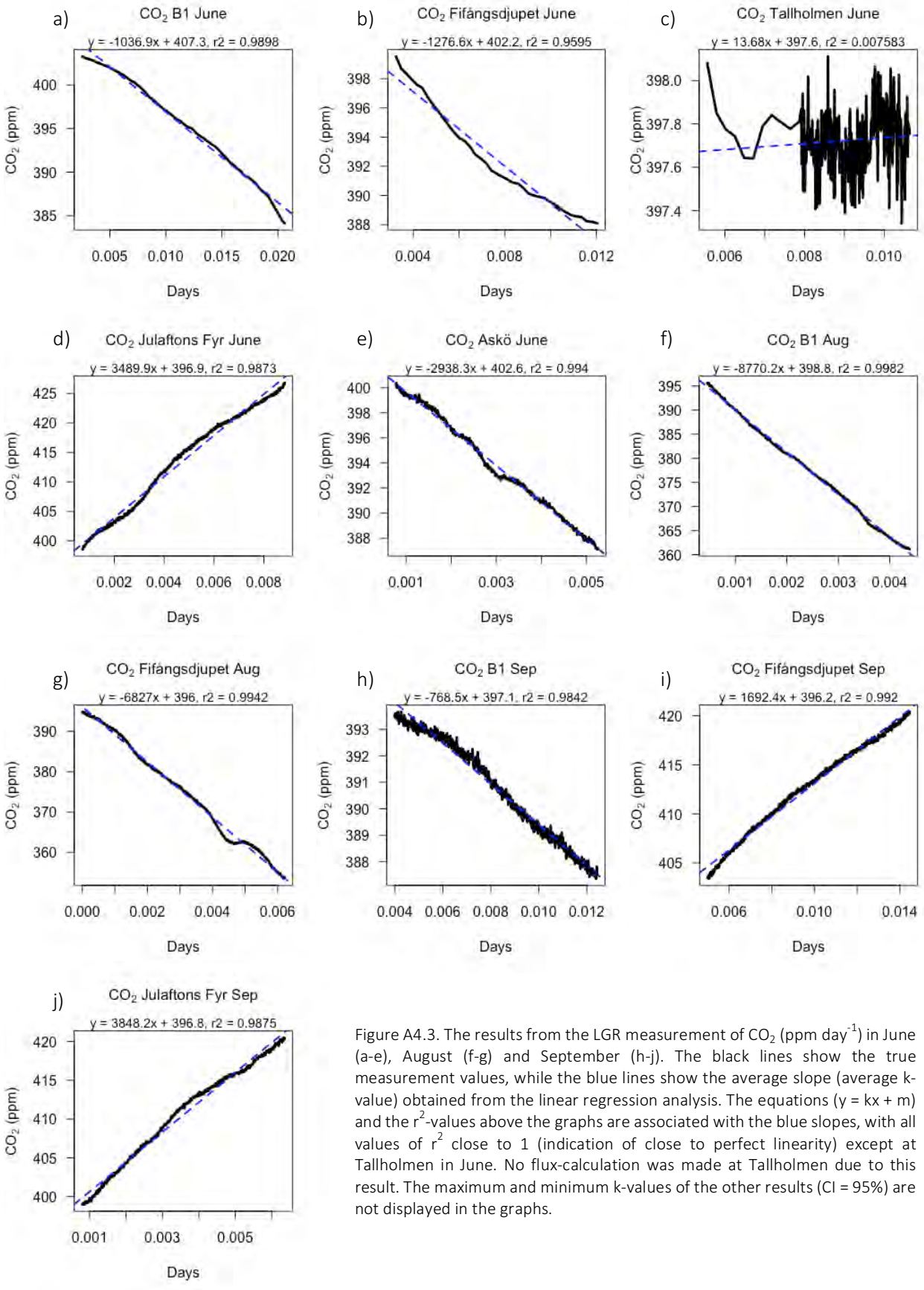

Figure A4.3. The results from the LGR measurement of CO_2 (ppm day^{-1}) in June (a-e), August (f-g) and September (h-j). The black lines show the true measurement values, while the blue lines show the average slope (average k-value) obtained from the linear regression analysis. The equations (y = kx + m) and the r^2-values above the graphs are associated with the blue slopes, with all values of r^2 close to 1 (indication of close to perfect linearity) except at Tallholmen in June. No flux-calculation was made at Tallholmen due to this result. The maximum and minimum k-values of the other results (CI = 95%) are not displayed in the graphs.

Appendix 5

A5.1 Hypothesis 2.1: ebullition *in situ* at Fifångsdjupet

The method to calculate the number of bubbles sec^{-1} $site^{-1}$ needed to reach to the mixed layer are presented here. The concentration in the surface water at Fifångsdjupet was 18 ± 1.9 nM in June and 22 ± 2.5 nM in August. Therefore, the concentration of a steady-state was set to 20 nM in the calculation. Assuming a steady-state, the bubble CH_4 input to the mixed layer will be the same as the output of CH_4 from the mixed layer. To simplify the calculation, the only output considered to be required was the water-air-flux. Oxidation was not considered as a CH_4 output since the decrease of CH_4 in the incubation experiments was considered to be negligible. A lateral transport of CH_4 out from the area was assumed to be equal to the amount in transport into the area and was neglected as well. The flux was therefore recalculated as CH_4 emissions (moles day^{-1}) for a water surface covering 7 km^2 (2 x 3.5 km, the area of Fifångsdjupet which included the seepage sites at Tallholmen):

$$E = \frac{(F*10^{-3}) * A}{M} \quad \text{(eq. A5.1)}$$

E = CH_4 emission (moles day^{-1})
$F*10^{-3}$ = results of the CH_4 water-air-flux (g m^{-2} day^{-1})
*A = area (m^2) of the water surface at Fifångsdjupet (2000*3500 m)*
M = molecular weight of CH_4 (16 g $mole^{-1}$)

Secondly, the number of moles of CH_4 per bubble was calculated. This was done for bubble diameters of d = 2 mm, d = 3 mm, d = 4 mm, d = 5 mm and d = 6 mm and where the pressure was assumed to be 2.5 bars at the seafloor of 24 m depth, with a temperature of 7°C and with assumption that the bubbles dissolved completely in the mixed layer:

$$n_x = \frac{P*V_x}{R*T} \quad \text{(eq. A5.2)}$$

n_X = number of moles of CH_4 per bubble with x diameter
P = pressure at the seafloor (Pa)
V_X = volume of the bubble with x diameter (m^3)
*R = 8.314 (Pa * m^3) (moles * K)$^{-1}$*
T = temperature at the seafloor (K)

Thereafter, the total number of bubbles with x diameters reaching the mixed layer per was calculated using the CH_4 emission as CH_4 input:

$$y = \frac{E}{n_x} \quad \text{(eq. A5.3)}$$

y = total number of bubbles day-^{1}

Thirdly, the number of bubbles sec^{-1} $site^{-1}$ reaching the mixed layer was calculated:

$$y_S = \frac{y}{s*24*60*60} \quad \text{(eq. A5.4)}$$

y_S = total number of bubbles sec^{-1} $site^{-1}$
s = total number of sites (600)

Lastly, the total seepage flow of bubbles sec^{-1} $site^{-1}$ was calculated:

$$y_T = \frac{y_S}{f} \quad \text{(eq. A5.5)}$$

y_T = total seepage flow (bubbles sec^{-1} $site^{-1}$)
f = fraction of number of bubbles reaching the mixed layer (0.04)

A5.2 Calculation in hypothesis 2.2: ebullition at shallower areas with lateral input of surface waters to B1

The isotope composition of the fluxes was calculated to test hypothesis 2.2 too see if the flux compositions deviated from the composition of the surface waters. The calculation was made with the equation:

$$\delta^{13}C_F = \frac{\delta^{13}C_{TOT} - \delta^{13}C_X * f_X}{f_F} \quad \text{(eq. A5.6)}$$

$\delta^{13}C_F$ = calculated isotope composition (‰) of the flux
f_F = fraction of the CH_4 moles in the chamber added by the flux (calculated from the measured concentrations)
$\delta^{13}C_X$ = measured isotope composition (‰) in the first air sample obtained from the chamber (figure 11)
f_X = fraction of the CH_4 moles contained in the chamber at the time when the first air sample was obtained
$\delta^{13}C_{TOT}$ = measured isotope composition (‰) in the second air sample taken from the chamber (figure 11)

The chambers were considered as closed systems with CH_4 input only from flux from the water below. The surface water was seen as an open system with CH_4 input from the surrounding water, leading to a stable value of isotope composition throughout the measurement time. Therefore, the $\delta^{13}C_F$ values were compared with the isotope composition of the surface water to obtain the difference in isotope composition ($\Delta^{13}C_{CH4}$). In figure 18, the various parameter in equation A5.6 can be distinguished.

A5.3 Flux vs. day time/night time in Hypothesis 2.2: ebullition at shallower areas with lateral input of surface waters to B1

The fluxes from the chamber sites were grouped and used in the testing of hypothesis 2.2, where it was thought that ebullition could occur at the shallow sites of Julaftons Fyr and the chamber sites. No relationship between day time/night time and amount of flux were noted as presented in figure A5.3.1. In June, the fluxes occurring during only night time in group N were lower than the ones during day time. However, in September the opposite was seen. No measurements were made only during night time in August.

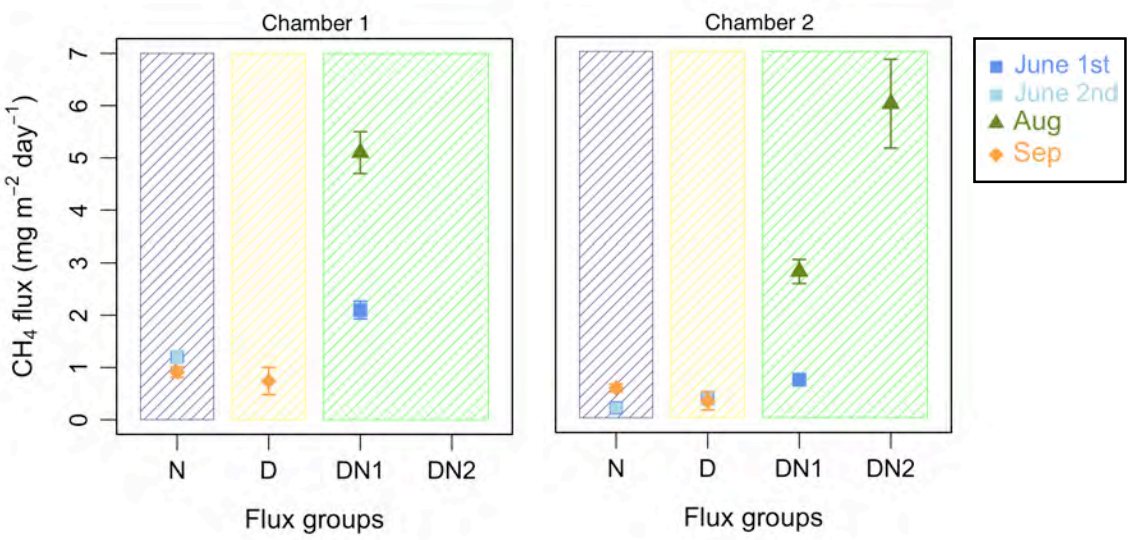

Figure A5.3.1. Graphs of the CH_4 fluxes (mg m^{-2} day^{-1}) at chamber 1 to the left and chamber 2 to the right in the grouped days N (night only), D (day only), DN1 and DN2 (day and night). June 1st = the first measurement made in June (Mon - Tues), June 2nd = the second measurement made in June (Wedn - Thurs).

A5.4 Leakage suspicion

Here are further explanation regarding the assumption that there might have been leakage from chamber 2 in August in group DN2. There was a heavier composition found in the chamber at day 2 (3rd sampling) compared to day 1 (2nd sampling) (figure 11), which contradicts the other results of continuingly lighter composition with time. If leakage had occurred, that would in return provide skewness in the results in figure 17 in the discussion regarding hypothesis 2.2, where the results showed of heavier composition of the CH_4 flux than of CH_4 in the surface water. However, indication of leakage is not seen when observing the concentration results from each day (Appendix 4: figure A4.1: CH_4: chamber 2), where the concentration was ~ 3 times as high at day 2 (141 ppm) compared to day 1 (44 ppm). It was therefore calculated according to the equation below an estimation of the amount of leakage that could have occurred if only considering the isotope composition:

$$\delta^{13}C_{TOT} = \delta^{13}C_Y * f_Y + \delta^{13}C_X * f_X + \delta^{13}C_Z * f_Z \qquad \text{(eq. A5.7)}$$

$\delta^{13}C_{TOT}$ = the average isotope composition (‰) in the chamber at day 2 (-58.6‰)
$\delta^{13}C_Y$ = isotope average composition (‰) in the chamber at day 1 (-59.5‰)
f_Y = fraction of the CH_4 moles in the chamber at day 1 (0.30)
$\delta^{13}C_X$ = isotope average composition (‰) of the atmosphere in August (-52.7‰)
f_X = fraction of the CH_4 moles added from a possible leakage, i.e., moles added from the atmosphere (tested)
$\delta^{13}C_Z$ = the calculated flux isotope composition (‰) from day 0 - 1 at chamber 2 in August (group DN1 = -59.8‰)
f_Z = fraction of the CH_4 moles added the flux (tested)

The chamber air at day 1 contributed with 30% of the total number of moles within the chamber at day 2, according to the concentration results (44 ppm/141 ppm * 100). The fraction added from the atmosphere and the flux (assuming same flux composition as calculated for day 0-1) were tested. When testing various contributing fractions, is seen that approximately 55% could have been added from the flux and 15% from the atmosphere. This means that is it possible that 15% of the chamber air could have been leaked between day 1 – 2 at chamber 2 in August. If that were the case, then the

concentration (ppm) measured at day 2 would have been ~ 15% higher if no leakage had occurred. This would have provided ~ 160 ppm in the chamber at day 2 instead of 141 ppm. That would in return have provided a total flux at chamber 2 in August of 5.2 mg m^{-2} day^{-1} instead of the 4.4 mg m^{-2} day^{-2}, presented in figure 11. This result seems fairly reasonable and the assumption was thereby that leakage could have occurred sometime between day 1-2 at chamber 2 in August.

Appendix 6

The measurement results of the CH_4 and CO_2 concentrations (ppm) from the LGR measurements were plotted against each other and presented in figure A6 below.

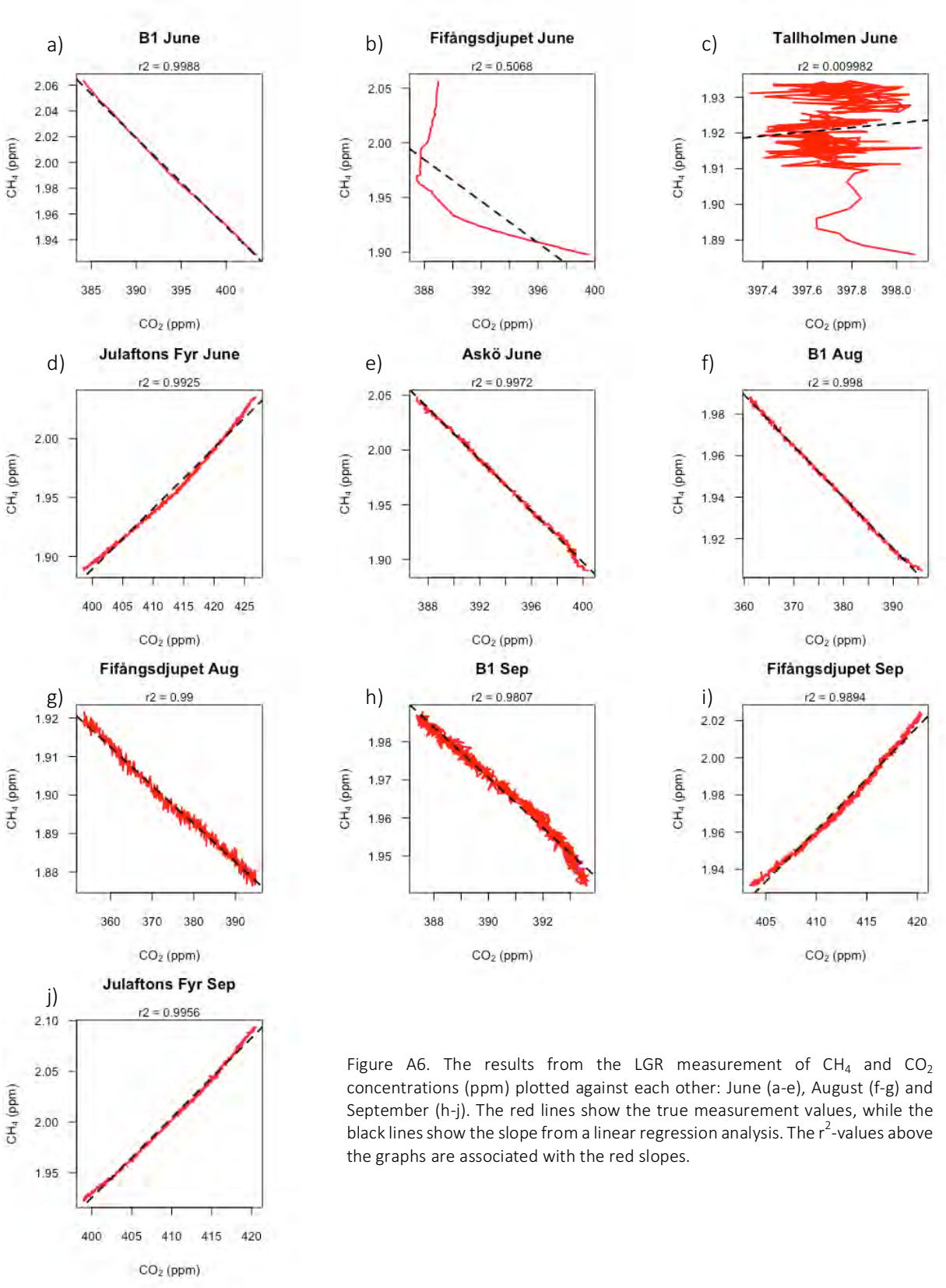

Figure A6. The results from the LGR measurement of CH_4 and CO_2 concentrations (ppm) plotted against each other: June (a-e), August (f-g) and September (h-j). The red lines show the true measurement values, while the black lines show the slope from a linear regression analysis. The r^2-values above the graphs are associated with the red slopes.